CHAPTER 3

RESULTS AND DISCUSSION

This chapter consists of three parts. The development of FI-on-line preconcentration procedure based on molecular sorption was mainly concerned. The preconcentration efficiency for determination of some trace elements using knotted and serpentine reactors was firstly mentioned. In the second part, the utilizing of knotted reactor for preconcentration and determination of chromium in water samples was described. In the last section, the novel column reactor was proposed for preconcentration of chromium (VI). Its preconcentration efficiency in comparison with the knotted reactor was investigated and discussed.

3.1 A Comparison of Enrichment Factor of Knotted and Serpentine Reactors Using Flow Injection Sorption and Preconcentration for the Off-line Determination of Some Trace Elements by Inductively Coupled Plasma Mass Spectrometry

Since the first application of the on-line sorption of neutral metal complexes onto the inner wall of a PTFE tube knotted reactor (KR) was proposed by Fang and co-workers in 1994 [11,12], the KR has been widely accepted as a trouble free and very effective sorption medium. The KR was made by tying the tubing into interlaced

knots, the KR creates increased secondary, radial flow in the stream, thus resulting in the creation of strong centrifugal forces, which, in addition to the hydrophobic nature of the PTFE surface, facilitates the sorption of the neutral complexes onto the interior surface of the KR [11,13].

Since the sorption mechanism is mainly effected by the secondary flow creation, the geometrical dimension of the reactor is considered as an important parameter influenced the preconcentration efficiency. Only three configurations namely, a straight conduit, a coiled reactors and a KR (all made from 100 cm long, 0.5 mm i.d. PTFE tubing) had been examined and compared on their preconcentration efficiencies for the FI on-line sorption preconcentration approach [11]. Among the three configurations tested, the KR showed higher sensitivity than those obtained by the coiled reactor and the straight conduit. At present, no study exists to compare the preconcentration efficiency obtained between the knotted with any reactors for sorption preconcentration system.

The serpentine reactor (SR) is one of the most attractive reactor which provides the secondary flow pattern as a result of its geometry [46,47]. The SR is preferable used as a connecting tubes in liquid chromatography. The SR described by Katz and Scoth [46,48] has a sine wave geometry (single plane, in two-dimensions ~). In a serpentine tube the velocity of liquid is continually changing in direction, which periodically reverses configuration have superior radial transport properties. These properties can promote a secondary flow pattern as occurred in the KR which ultimately provide an effective preconcentration capability as well as the KR.

In addition, recently, Waiz *et al.* [49] have studied the band dispersions observed in tubular conduits of different overall geometry. Straight, coiled and various types of serpentine and superserpentine geometries of open tubular reactors were studied and compared with the knotted reactor. The observed dispersion per unit residence time of superserpentines performs substantially better than a serpentine or simple coil, but not as well as a knotted reactor. The performance of the superserpentine and the knotted reactors was nearly identical.

It is, therefore, beneficial to study and compare the preconcentration efficiency between the knotted and the serpentine reactors for an FI sorption preconcentration system for appropriate preconcentration of non-charged metal complexes. In this section the preconcentration efficiency expressed in term of enrichment factor (EF) of the knotted and the serpentine reactors was investigated. The preconcentration system was demonstrated for the determination of some trace metals namely, Cr(VI), Ni(II), Co(II), Cu(II), Zn(II), Mo(VI), Cd(II), W(VI) and Pb(II) *via* complexation with ammonium pyrrolidinedithiocarbamate (APDC) and sorbed on the inner wall of the reactors (KR and SR). The concentrated metal complexes were subsequently eluted by 2%(v/v) nitric acid. The preconcentrated trace metals were finally off-line determined by ICP-MS.

Establishment of experimental parameters for optimization was initiated by investigating the optimum length of the KR for preconcentration. The SR having 8-shaped configuration at the same optimum length as that of the KR was then prepared. The 0.5 mg/l multi-element standards solution was used throughout the optimization steps. The EF form the KR and the SR at the same optimum conditions were compared and discussed in more details as follows.

3.1.1 Manifold Design and Operation Sequences

The manifold used and its operational sequences were shown in Fig. 2.1 and Table 2.3, respectively. In general, two basic steps were included in the operational sequence for an FI on-line KR sorption preconcentration. One is the on-line formation of neutral analyte complex and its subsequent sorption on the inner wall of the KR, the other is on-line elution of the sorbed analyte complex for determination Although the ICP-MS is the most sensitive, accurate and reliable trace multi-element measurement detector, it has low tolerance limit to the total dissolved salt (TDS) (0.2% m/v) and polyatomic interferences [50-53]. Accordingly, a washing step (rinse reactor) before elution is necessary and employed for the FI KR sorption preconcentration ICP-MS, due to the residual solution in the KR after loading the sample may contain high contents of dissolved salts and interfering species [54]. Introduction of such residual solution with the eluate into the ICP-MS system could block the sampling cone and produce interferences. Thus, the rinsing step was designed and incorporated into the operational sequences.

3.1.2 Optimization of Sample Acidity

The effect of sample acidity on the preconcentration of the element studied was investigated by using diluted nitric acid because of its compatibility with the ICP-MS. It was examined at a fixed sample (1.5 ml/min) and reagent (1.5 ml/min) flow rates and reagent concentration (0.1% w/v APDC). This effect was studied over the concentration of nitric acid range 0.0001-0.25 mol/l. As can be seen in Fig. 3.1, an optimum range of sample acidity of 0.0001-0.1 mol/l HNO_3 for the preconcentration of some trace metals was almost identical for all analytes under investigation. The

preconcentration efficiencies for all analytes decreased significantly as the sample acidity was over 0.1 mol/l HNO_3. Therefore, a sample acidity of 0.001 mol/l HNO_3 was selected in further experiments for the preconcentration and determination of all the trace elements studied.

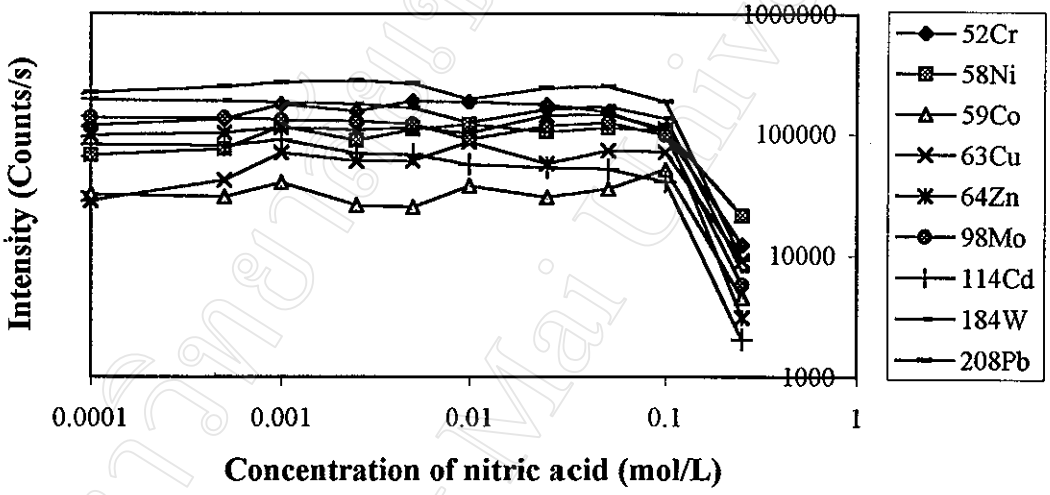

Figure 3.1 Effect of sample acidity using a KR on the signal intensity of a 0.5 mg/l multi-elemental standard.

3.1.3 Optimization of the Complexing Agent (APDC) Concentration

In most FI on-line KR sorption systems, the preconcentration of the analyte is achieved through on-line merging the sample with complexing reagent solution and ensuing sorption of the resultant neutral metal complex. By using the approach, a variety of complexing reagents have been studied for on-line formation of neutral metal complexes, including diethyldithiocarbamate (DDTC) [12, 55-56], ammonium pyrrolidinedithiocarbamate (APDC) [33, 40, 43, 53, 57-66],

diethyldithiophosphate (DDPA) [67-69], 8-hydroxyquinoline (8-HQ) [59, 62, 70], 1-phenyl-3-methyl-4-benzoylpyrazolone-5 (PMBP) [62, 71], 2-nitroso-1-naphthol-4-sulfonic acid (NNA) [62], 2-(5-bromo-2-pyridylazo)-5-diethylaminophenol (5-Br-PADAP) [72,73] and dithione [74]. Both DDTC and APDC are widely used because they are capable of forming complexes with a wide range of metal ions ,which suitable for multielement determination, although offer low selectivity.

It is known that DDTC is unstable in acid solution with a half-life of only 0.3 s at pH 2 [75]. For this reason, DDTC solution should be prepared in basic buffer medium (e.g. $NH_3 \bullet H_2O$-NH_4Oac, pH 9.0) [11, 12, 76, 77]. By comparison the stability of DDTC with that of APDC at various pH values, it is clear that APDC is much more stable in acid solution than DDTC with half-life values of 32 min, 59 min, 2 h, 20 h, 9 d and 170 d at pH <2, 3, 4, 5, 6, 7 and 7.3 respectively [78]. Therefore, APDC solution can simply be prepared in deionized water [63,78]

The APDC was, thus, chosen as complexing agent in this work due to its solubility both in water and acidic medium in which the studied metal complex was formed. The APDC has a structure formula structure as show in Fig. 3.2.

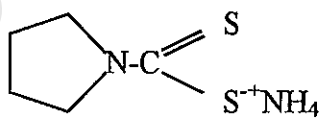

Figure 3.2 The structural formula of APDC

There are one N and two S in its molecule. The reaction between heavy metal ions and the chelator are the total results of ammonication and sulfuration [cited

in 74]. Many heavy metal ions are inclined to form particular sulfides, which are able to be extracted by APDC. These ions often have d electron orbit unfilled (such as Cu, Co, Cd, Ni, Pt, etc.) or have 10 d electrons (such as Zn, Pd, Bi, Hg, In, etc.) [cited in 74]. That is why APDC was widely used. According to the hard and soft acid-base theory [80], when heavy metal ions M^{n+} (soft acid) coexist with H^+ (hard acid), the soft base S is inclined to chelate with M^{n+} while the hard base N are to be occupied by H^+. Therefore, APDC is preferably prepared in low pH condition. The benzene ring in the APDC molecule do good to the absorbance of chelate complex to the inner wall of KR for its non-polarity [81], which will also cause easier deposition of chelator molecules on the inner wall of the KR when the chelator concentration is suitable.

Consequently, the APDC concentration should be optimized. The influence of APDC concentration in the range of 0.001-1.0% (w/v) was then evaluated when the sample flow and reagent flow rates were kept constant at 1.5 ml/min.

As shown in Fig. 3.3, an increase in the signal intensities with an increase in the APDC concentration was observed for Pb and Zn. Some elements (Cd, Co, Cu, Cr, Ni) had a slight maximum intensities at 0.1% (w/v) APDC, meanwhile others (Mo, W) showed the steady signal over the range of study. Because of the benzene ring, the APDC molecules might completed with the chelate complex on the walls of KR when the concentration of APDC increased above 0.1% (w/v), causing the slightly decline of intensities of some detected metal ions (Cd, Co, Cu, Cr, Ni). Therefore, 0.1% (w/v) APDC was considered as the optimum complexing reagent concentration which having the efficiency of preconcentration for all elements studied.

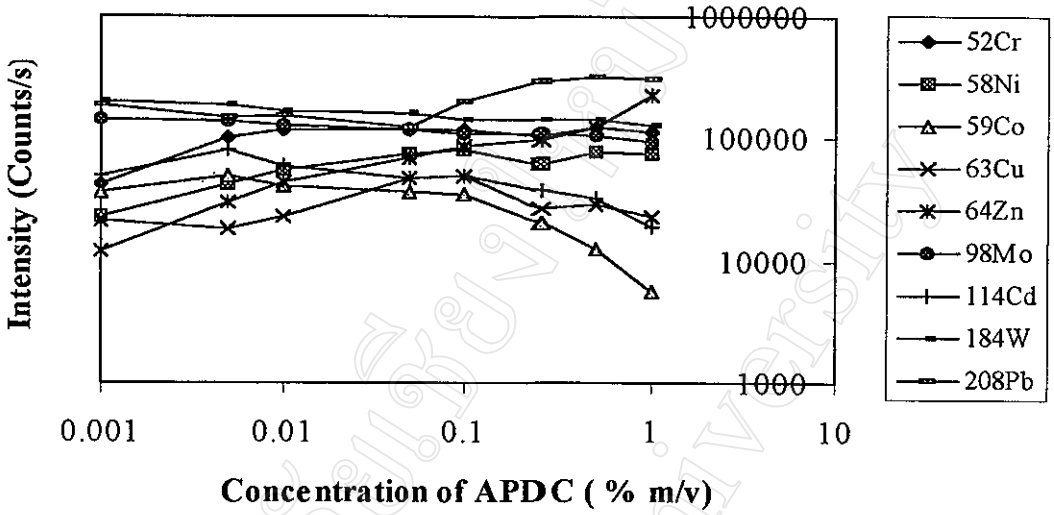

Figure 3.3 Effect of APDC concentration using a KR on the signal intensities of a 0.5 mg/l multi-elemental standard.

3.1.4 Optimization of Sample and the APDC Flow Rate

The effect of the sample flow rate was investigated on the KR at a fixed reagent flow rate of 0.45 ml/min. The sample flow rate was varied over the range of 0.23-5.0 ml/min. The effect of reagent flow rate was further tested at a fixed sample flow rate of 4.0 ml/min while the reagent flow rate was varied from 0.25 to 5.0 ml/min. An optimum ratio of 2.0-2.5 between the flow rates of sample and chelating reagent was observed. The conditions and the values of the variables adopted were given in Table 2.3.

3.1.5 Optimization of the KR Length

The influence of the KR length on the preconcentration of all elements was examined over the range of 25-200 cm for a fixed preconcentration period of 60 s,

at a constant sample flow rate of 1.2 ml/min and reagent flow rate of 0.5 ml/min. As illustrated in Fig. 3.4, the intensity for most elements (except Co, Zn) was found to increase linearly with increasing in KR tubing length up to 100 cm. At longer tubing length, the signals were gradually approached a constant value. For Co, the maximum intensity was observed at the KR length of 75 cm. The signal decreased with increasing the KR length. The maximum intensity of Zn was observed at the KR length of 150 cm. These results were evidence of the competition between the APDC complexes of the separate analytes for the achieve sites on the walls of the KR. The most important factors in this content are the kinetic stability of the analyte-APDC complex and the strength of sorption bonding to the KR in acid solution [53]. For the above results, the KR length of 150 cm was selected as an optimized length for further studies, which has sufficient capacity to accommodate all APDC complexes.

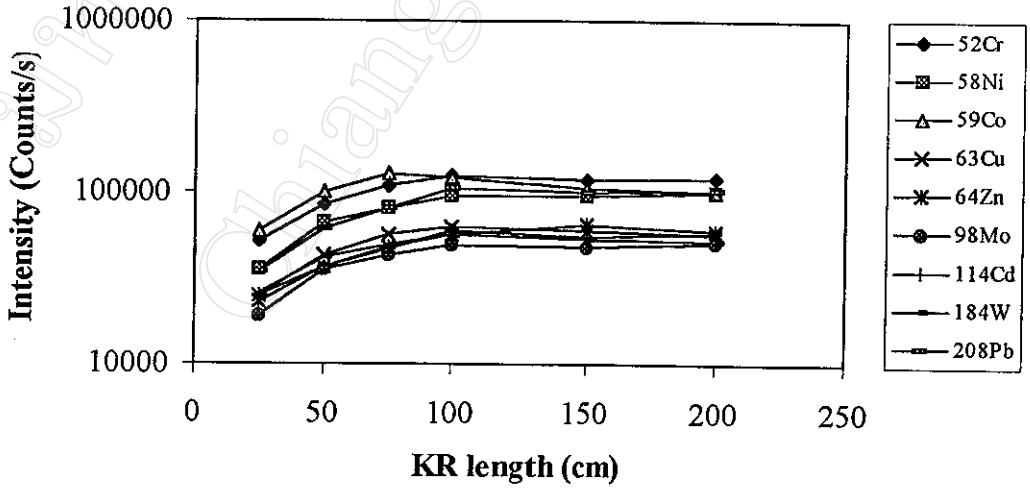

Figure 3.4 Effect of KR length on the signal intensity of a 0.5 mg/l multi-elemental standard.

3.1.6 Optimization of the Sample Loading Time

The optimization of the preconcentration time, or sample loading time, is interesting in relation to the reaction mechanism. It was expected to obtain a straight line relationship until the breakthrough of the KR was reached.

The effect of sample loading time was evaluated in the range from 30 to 300 s at a constant sample flow rate of 1.2 ml/min, reagent flow rate of 0.5 ml/min and the KR length of 150 cm. As can be seen from Fig. 3.5, the analyte intensity increased almost up to 120 s, leveling off with further increases in loading time. In contrast with Co, after the preconcentration time of 120 s, the intensity remained practically constant above this value and up to 300 s. Thus, the sample loading time of 120 s was chosen for further experiments as compromise between the medium consumption, sufficient sensitivity and frequency of sample throughput.

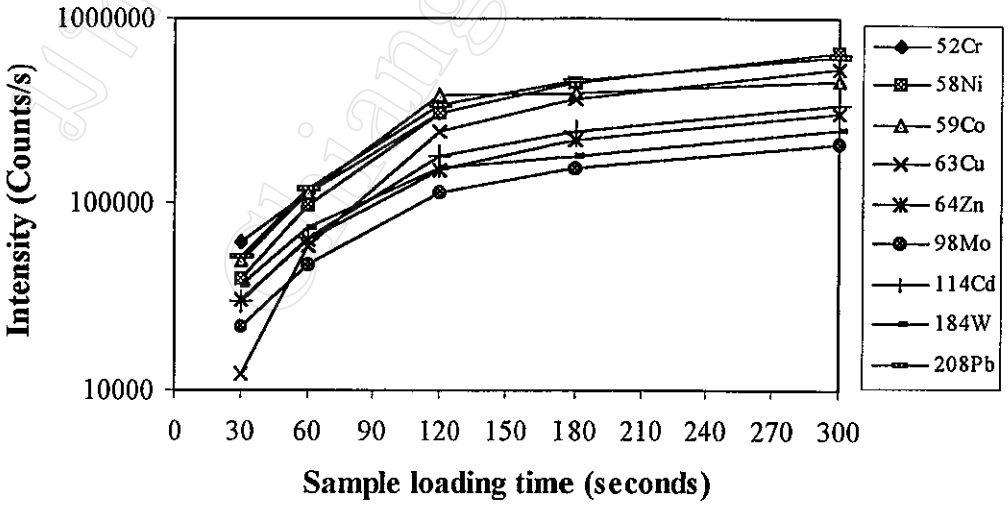

Figure 3.5 Effect of sample loading time using a KR on the signal intensity of a 0.5 mg/l multi-elemental standard.

3.1.7 Rinsing the KR

The rinsing step aims at removing all non-adsorbed or weakly adsorbed constituents of the matrices without stripping the analyte from the KR. This step of the preconcentration procedure is of particular significance for the analysis of samples with a high matrix concentration, because the introduction of such a residual solution with the eluate into the ICP-MS system could block the sampling cone and produce interferences.

In the literature, rinsing with doubly deionized water (DDIW) produced a broad signal with lower sensitivity and poorer precision than with dilute nitric acid [65]. Accordingly, dilute nitric acid was registered for rinsing.

Depending on the stability of the complexes formed and the acidity of the rinsing solution, the more weakly adsorbed complexes were removed while the more strongly adsorbed complexes were still retained on the reactor. Fig. 3.6 shows the effect of nitric acid concentration in the rinsing solution on the preconcentration system. The signal intensity appears to be a increase between 0 and 0.02% for Co, Mo, Cu and Ni, after which the intensity decreased and remained constant above 0.1% and up to 0.2%. The other elements (Cr, Zn, Pb, Cd, W), the signal intensities decreased with increasing the nitric acid concentration up to 0.06%. The signal intensities slightly increased and remained constant with further increase in HNO_3 concentration. From the above results, it is probably pointed out that the APDC complexes of Co, Mo, Cu and Ni are stronger adsorbed on the KR than those of Cr, Zn, Cd, W and Pb. This evidence were supported by the enrichment values as shown in Table 3.2 in the Section 3.1.10. As a compromise between the rinsing efficiency

and the prevention of stripping from the reactor for all elements studied, a 10 s rinsing with 0.02% (v/v) HNO_3 at a flow rate of 2.85 ml/min were adopted.

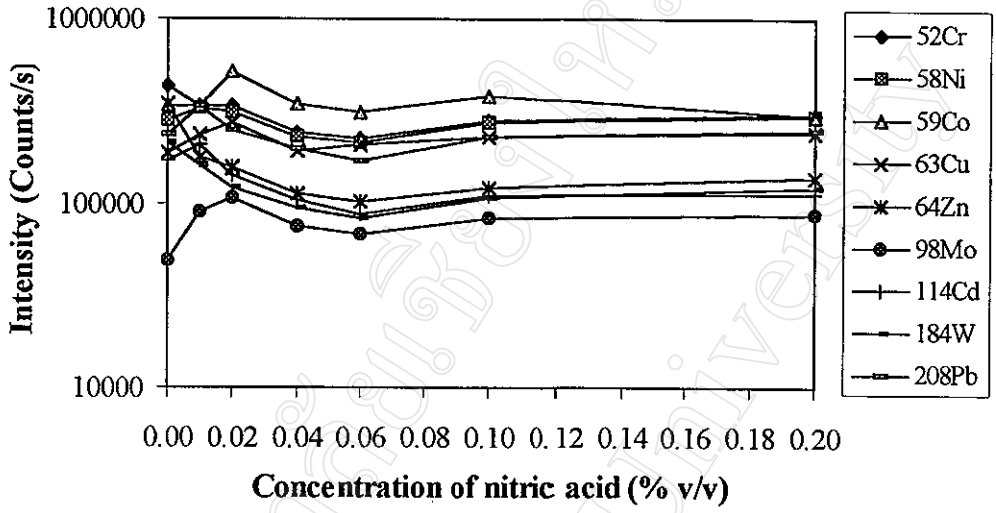

Figure 3.6 Effect of rinsing nitric acid concentration using a KR on the signal intensity of a 0.5 mg/l multi-elemental standard.

3.1.8 Elution

An appropriate eluent should not only effectively elute the adsorbed analyte but should be favorable for the subsequently detection. In this work, the ICP-MS, which allows multielemental analysis was used as a detector. For this reason, dilute nitric acid (2% (v/v)) which conventional used and provided low background for ICP-MS determination was employed as the eluent. Since the ICP-MS needs sufficient volume of the analyte solution (approximate 2 ml) per determination with conventional off-line detection, the 5 ml of eluate was collected in a test tube for obtaining sufficient volume to introduce into the ICP-MS system for duplicate determinations.

3.1.9 Summary of the Optimum Conditions

The optimum conditions obtained by using the so-called univariate method as described earlier in sections 3.1.2-3.1.8 for the FI system are summarized in Table 3.1.

Table 3.1 Conditions used for determination

Parameter studied	Optimum conditions
Sample	Metal standard solution in 0.001 M HNO_3
Flow rate of sample	1.20 ml/min
Reagent	0.1% (w/v) APDC
Flow rate of reagent	0.50 ml/min
Washing solution	0.02% (v/v) HNO_3
Flow rate of washing solution	2.85 ml/min
Eluent	2% (v/v) HNO_3
Flow rate of eluent	3.30 ml/min
Length of KR and SR	150 cm (PTFE 0.35 mm i.d.)
Preconcentration time	120 s

3.1.10 Comparison of the Enrichment Factor of the FI Sorption and Preconcentration System on KR with that of Using SR

Based on the optimum conditions obtained in Section 3.1.5, a SR with a length of 150 cm was made. The EF of the KR and the SR under the same optimum conditions, as described in Sections 3.1.2-3.1.8, were evaluated, the results being compared in Table 3.2.

Table 3.2 EF of the FI sorption and preconcentration system using KR and SR

Isotope	Enrichment factor (EF)	
	KR	SR
^{52}Cr(VI)	11	6
^{58}Ni(II)	12	5
^{59}Co(II)	36	12
^{63}Cu(II)	13	5
^{64}Zn(II)	4	3
^{98}Mo(VI)	20	10
^{114}Cd(II)	10	5
^{184}W(VI)	8	4
^{208}Pb(II)	13	7

The EFs were calculated from the ratio of the analyte intensities with and without a preconcentration step, respectively. Without preconcentration, the reactors were not incorporated in the system. A higher preconcentration efficiency can be achieved with the KR as compared with the SR, comparing preconcentration units of equal reactor length (150 cm). It was found that the EF gained in the KR was higher than that in the SR for all analyte under investigation. The EF of 4-36 and 3-12 were achieved using KR and SR, respectively. Since the shape of the reactor has significant influence on the preconcentration efficiency in the system. It could be presumably indicated that the three dimensional configuration of KR created much

more stronger secondary flow pattern than those in SR. The KR should be preferable to use for the sorption preconcentration system.

3.2 Flame Atomic Absorption Spectrometric Determination of Chromium (VI) and Total Chromium in Water Samples by FI On-line Preconcentration System Using Knotted Reactor

Recently, the opportunity for the determination of chemical components in various natural samples has been increased especially in the research fields such as environmental chemistry and geochemistry. Chromium is one of the trace elements that has drawn attention in these fields.

Chromium exists in two oxidation states (III and VI) with different thermodynamic, kinetic, biochemical and toxicological behavior in natural water (see Section 1.2). For these reasons, the separate determination of the two species in environmental samples has become very important. Many methods for the determination of chromium in a sample containing both Cr(III) and Cr(VI) are based on the determination of Cr(VI) and total chromium, because of Cr(III) is kinetically inert [79].

In this section, the KR was extended to incorporated into the FI on-line preconcentration system for determination of chromium (VI) and total chromium in water samples. Chromium (VI) has been preconcentrated and separated from Cr(III) by adsorption of Cr(VI) via complexation with APDC on the inner wall of the KR. After elution of Cr(VI) with IBMK, it was analyzed by FAAS. Total chromium was

determined by FAAS after Cr(III) was converted to Cr(VI) by oxidation with potassium peroxydisulfate and then total Cr(VI) was concentrated as above. Cr(III) can then be calculated by subtracting Cr(VI) with the total chromium. This procedure was applied to several water samples for the determination of Cr(VI), Cr(III) and total chromium.

3.2.1 Manifold Design and Operational Sequences

Two main basic steps, preconcentration and elution, were involved. The washing step before elution was not included because FAAS provides higher tolerance limit to the residual solution than that of the ICP-MS. The manifold used and the operational sequences were exhibited in Fig. 2.2 and Table 2.4, respectively.

3.2.2 Optimization of the Condition Used for FAAS Instrument

The effect of burner height and flame condition were optimized at concentration of Cr(VI) and APDC were 0.5 mg/l and 0.2%(w/v), respectively. A KR of 100 cm with 60 s loading time was set. The height of burner for observation was varied between 0.3-0.7 cm. The results are shown in Table 3.3 and Fig. 3.7.

As shown in Fig. 3.7, the burner height at 0.3 cm gave highest sensitivity for chromium determination. This height was set and used throughout this study.

Air-acetylene flame which generally recommended for chromium determination was used. Flame condition was optimized by fixing the air aspiration rate (8.0 l/min) while acetylene aspiration rate was varied. The results are presented in Table 3.4 and Fig. 3.8.

Table 3.3 Effect of burner height for observation on Cr(VI) determination

Burner height (cm)	Peak height (cm)			Average (cm)	SD
0.3	3.15	3.00	3.10	3.08	0.076
0.4	4.45	4.55	4.75	4.58	0.153
0.5	3.70	3.80	4.00	3.83	0.153
0.6	2.35	2.50	2.45	2.43	0.076
0.7	2.25	2.35	2.35	2.32	0.058

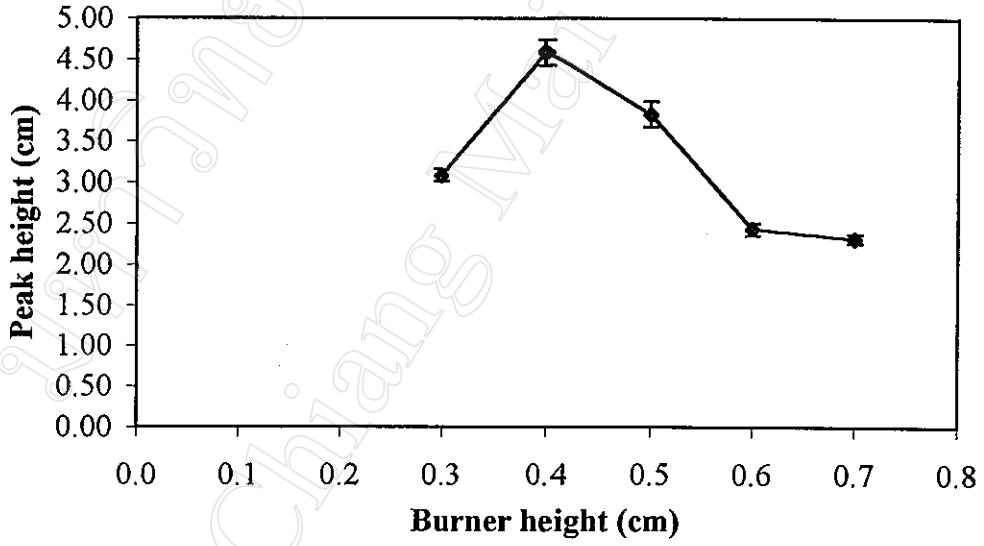

Figure 3.7 Effect of burner height for observation on Cr(VI) determination

Table 3.4 Effect of acetylene aspiration rate on Cr(VI) determination

Acetylene aspiration rate (l/min)	Peak height (cm)			Average (cm)	SD
2.3	5.34	5.34	5.34	5.34	0.000
2.4	5.71	5.75	5.81	5.76	0.050
2.5	6.19	6.25	6.19	6.21	0.035
2.6	6.15	6.15	6.20	6.17	0.029
2.7	6.45	6.45	6.40	6.43	0.029
2.8	6.40	6.40	6.50	6.43	0.058
2.9	6.50	6.50	6.50	6.50	0.000

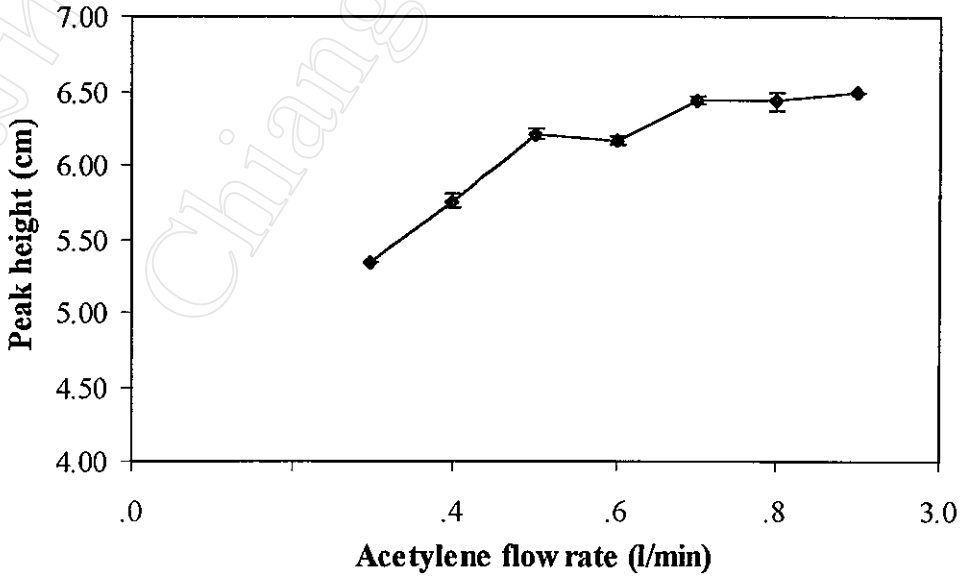

Figure 3.8 Effect of acetylene aspiration rate on Cr(VI) determination

The signal was found to increase with increasing the aspiration rate from 2.3-2.7 l/min. At higher flow rate, the signal was remained constant. In this way, acetylene aspiration rate of 2.7 l/min was chosen. Flame conditions were then set at 2.7 l/min acetylene and 8.0 l/min air, which were slightly leaner than those recommended. This measure was taken to compensate for the effect of the organic solvent (IBMK) introduced during elution, which served as additional fuel.

3.2.3 Optimization of the Sample Acidity, [HCl] and APDC Concentration, [APDC]

In this work, Cr(VI) was used as it is the chelate-forming species in acidic media. Since FAAS is not restricted only for HNO_3 as the ICP-MS, different types of acids namely HNO_3, H_2SO_4 and HCl were firstly investigated for acidity adjustment. The influence of acid types on the preconcentration of Cr(VI) with the concentration of APDC at 0.2% (w/v), 100 cm KR length and preconcentration time of 60 s was illustrated in Table 3.5 and Fig. 3.9.

Table 3.5 Effect of acidity type on Cr(VI) determination

Concentration of Cr(VI) (mg/l)	**Peak height (cm)**		
	H_2SO_4 (M)	**HCl (M)**	**HNO_3 (M)**
0.05	0.25	0.40	0.42
0.10	1.50	1.98	1.71
0.15	2.87	3.83	3.03
0.20	3.97	5.28	5.08
Regression equation	**Y=25.06x-0.985**	**Y=32.98x-1.25**	**Y=30.6x-1.265**
r^2	**0.9983**	**0.9980**	**0.9858**

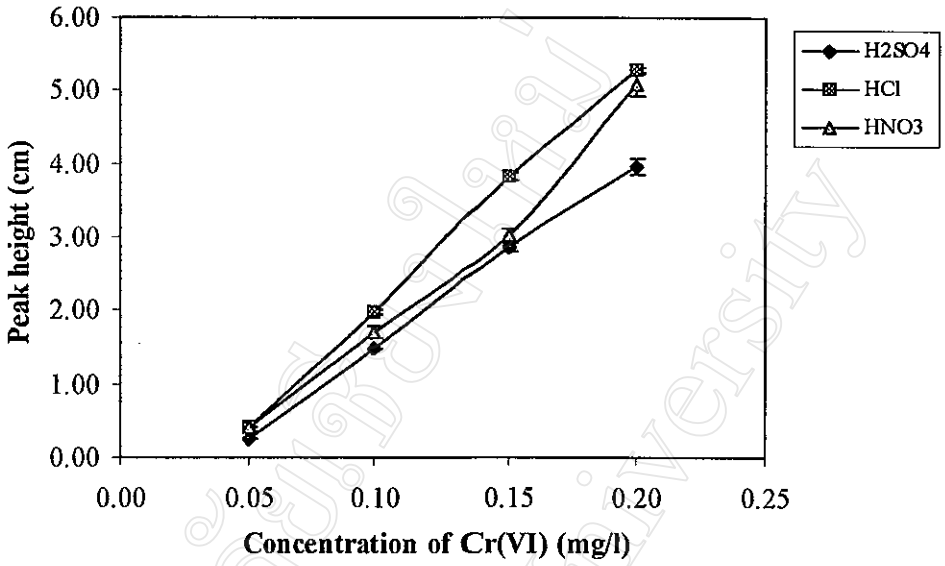

Figure 3.9 Effect of acidity type on Cr(VI) determination

Within the concentration range of 0.05-0.20 mg/l Cr(VI), sample solution in HCl exhibited better sensitivity (slope) than that in HNO_3 or H_2SO_4. Actually, HCl can be used as well as HNO_3 because they provide nearly the same sensitivity i.e., 32.98 and 30.60 cm/(mg/l), respectively. With respect to linearity of the calibration graphs Cr(VI) in HCl shows the better linearity (r^2 = 0.9980) than that in HNO_3 (r^2 = 0.9858). For these reasons, HCl was chosen to adjust the sample acidity throughout this work. The complexing agent, APDC, was continuously used in this section as a result of many benefits gained as previously discussed in Section 3.1.3.

The concentration of HCl, [HCl], and APDC, [APDC], were optimized by variable-size simplex method [Appendix A] in order to examine the optimum or near optimum conditions within a relatively small number of experiments. The results obtained thereby were shown in Fig. 3.10.

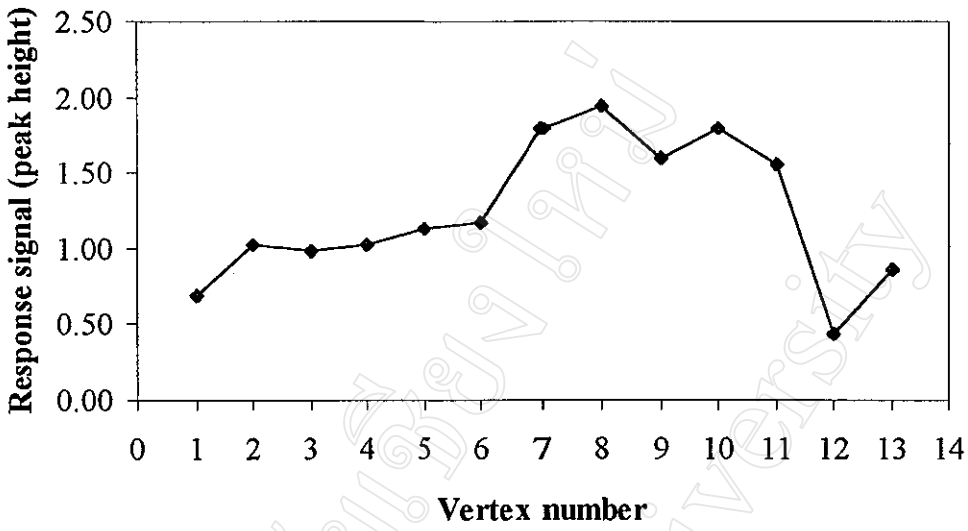

Figure 3.10 The relationship of response signal and the vertex number for optimization

As it is seen, the simplex procedure was performed smoothly, and the optimum conditions were found to be at a vextex number of 8, they were, [HCl]=0.15 M and [APDC]=0.2% (w/v). These conditions were employed in the following optimization steps.

3.2.4 Optimization of the Sample and the APDC Flow Rate

The influence of the flow rates of sample and APDC was investigated in the interval of 3-5 ml/min and 1-6 ml/min, respectively. The results were exhibited in Table 3.6 and Fig. 3.11.

Table 3.6 Effect of sample/APDC flow rate ratio on Cr(VI) determination

Sample/APDC flow rate ratio	Peak height (cm)			Average (cm)	SD
0.83	5.45	5.50	5.40	5.45	0.050
1.00	5.70	5.80	5.70	5.73	0.058
1.25	5.80	5.90	5.90	5.87	0.058
2.08	5.70	5.75	5.75	5.73	0.029
4.16	5.70	5.60	5.60	5.63	0.058

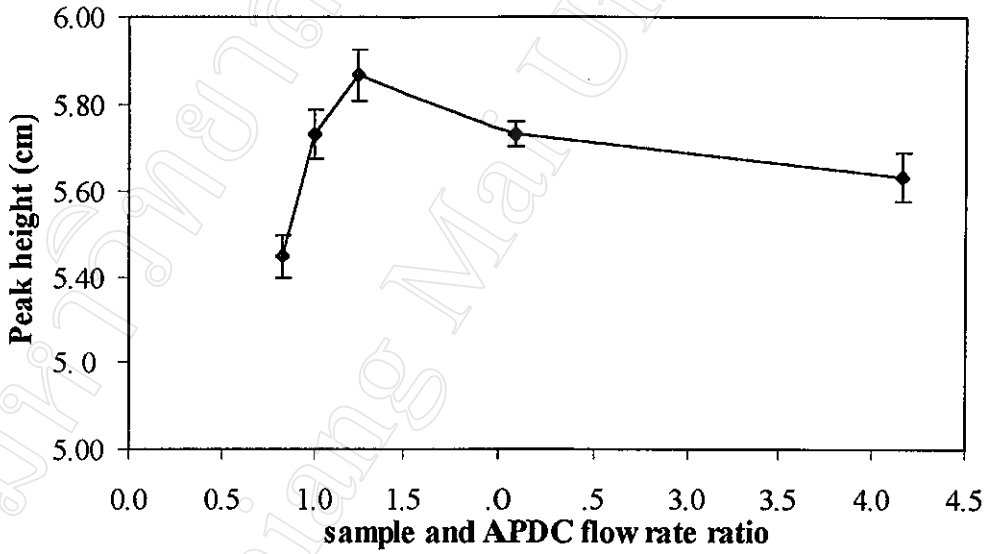

Figure 3.11 Effect of sample/APDC flow rate ratio on 0.10 mg/l Cr(VI) determination

It was shown that the signal was highest at a sample/APDC flow rate ratio of 1.25. Owing to low hydrodynamic impedance in the KR, the proposed sorption preconcentration system should allow the use of substantially higher sample loading flow rates to achieve higher concentration efficiencies. Therefore, a high

sample loading flow rate of 5.0 ml/min was employed. For keeping a sample/APDC flow rate ratio in the optimum conditions at 1.25, an APDC flow rate of 4.0 ml/min was chosen.

3.2.5 Optimization of the KR Length

The effect of KR tubing length on the preconcentration of Cr(VI) was examined at a constant sample flow rate of 5.0 ml/min and reagent flow rate of 4.0 ml/min in the range of 50-150 cm for a fixed preconcentration time period of 60 s. The results are shown in Table 3.7 and Fig. 3.12.

Table 3.7 Effect of KR length on Cr(VI) determination

KR tubing length (cm)	Peak height (cm)			Average (cm)	SD
50	6.50	6.40	6.55	6.48	0.076
75	7.05	6.90	6.90	6.95	0.087
100	7.70	8.00	7.80	7.83	0.153
125	8.10	8.10	8.10	8.10	0.000
150	8.10	8.10	7.85	8.02	0.144

As illustrated in Fig. 3.12, the signal of Cr(VI) increased with increasing KR tubing length from 50 to 125 cm but slightly leveled off from 125 to 150 cm. These results could be explained in term of adsorption eficiency and dispersion. The peak height of the transient analyte signal depends not only on adsorption efficiency but also on analyte dispersion during elution and transport of eluate. High adsorption efficiency and low analyte dispersion would produce high

peak height of the transient signal. A shorter KR provided insufficient contact of the analyte complex with the KR, and hence less adsorption efficiency, resulting in a lower peak height. On the other hand, analyte dispersion was less in a shorter KR during elution and analyte transport to the FAAS system, leading to a higher peak height. In contrast, a longer KR offered higher adsorption efficiency and higher analyte dispersion. Below a KR tubing length of 125 cm, the adsorption efficiency dominated the signal intensity, so the peak height increased with increasing in KR tubing length. However, over KR length of 125 cm, the analyte dispersion might control the signal; therefore the peak height decreased as KR tubing length increased. Based on the above results, a KR tubing length of 125 cm was selected.

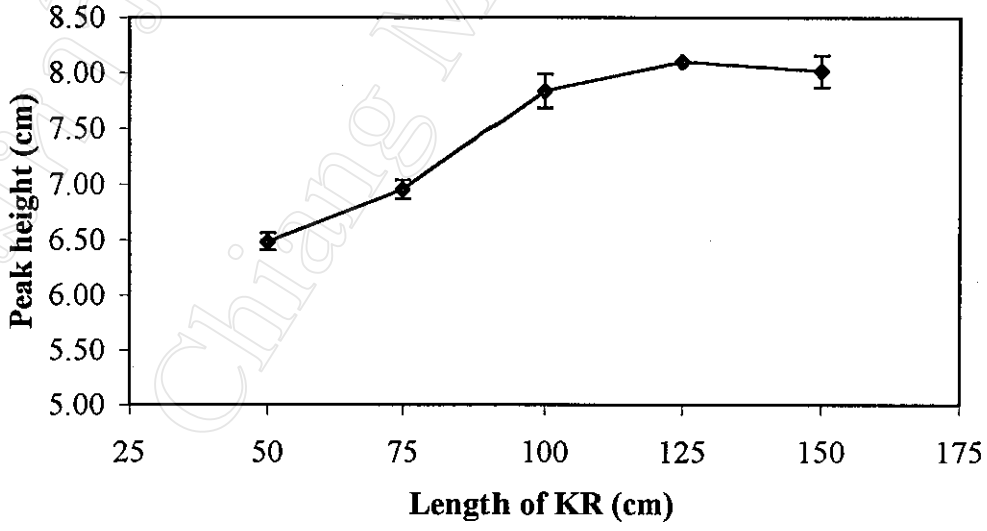

Figure 3.12 Effect of KR tubing length on 0.10 mg/l Cr(VI) determination

3.2.6 Optimization of the Sample Loading Time

The effect of sample loading time on the preconcentration of Cr(VI) was evaluated at a constant sample loading flow rate of 5.0 ml/min and reagent flow rate of 4.0 ml/min with the KR length of 125 cm in the range from 30 to 240 s. The results are shown in Table 3.8 and Fig. 3.13.

Table 3.8 Effect of sample loading time on Cr(VI) determination

Sample loading time (s)	Peak height (cm)			Average (cm)	SD
30	0.81	0.82	0.84	0.82	0.015
60	1.55	1.54	1.62	1.57	0.044
90	2.11	2.07	2.11	2.10	0.023
120	3.20	3.40	3.30	3.30	0.100
150	3.65	3.50	3.40	3.52	0.126
180	3.80	3.90	4.00	3.90	0.100
210	4.50	4.40	4.45	4.45	0.050
240	5.10	5.20	5.15	5.15	0.050

As can be seen in Fig. 3.13, it was found that the peak height increased almost linearly up to 120 s, after which it increased with lower sensitivity (slope), presumably as a result of an insufficient capacity of the KR and/or a chromatographic effect with the adsorbed analyte being partially leached by further sample [11, 16, 63]. Thus, a 180 s loading time was chosen as a compromise between medium sample consumption, sufficient sensitivity and sampling throughput.

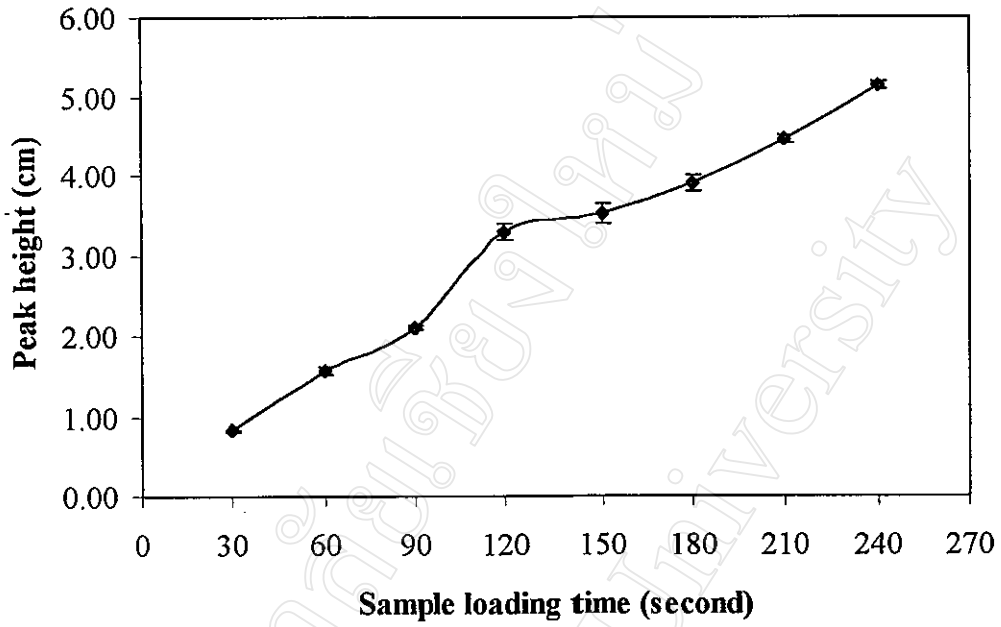

Figure 3.13 Effect of sample loading time on 0.10 mg/l Cr(VI) determination

3.2.7 Analyte Elution and Eluate Introduction

The inclusion of organic solvents in the sample may enhance the sensitivity of FAAS both through a decrease of surface tension of the sample solution, which results in finer nebulization, and through an increase in flame temperature compared to simple aqueous solutions. Therefore, isobutyl methyl ketone (IBMK) which was often used as the eluent in FI on-line KR sorption preconcentration for FAAS [63] was selected to elute the Cr(VI)-PDC complexes. The advantages of IBMK over other organic solvents such as methanol and ethanol for elution due to a more intensive organic solvent effect and partially to a decrease in dispersion owing to the used of a water immiscible solvent [11, 12]. Nevertheless, the advantages of using IBMK as eluent by far outweighed the disadvantages of using an organic

solvent unsuitable to be directly delivered through peristaltic pump tubings (i.e. a displacement bottle had to be implement). Therefore, in this work a HPLC pump was used in stead of a peristaltic pump to handle the IBMK.

The flow rate of the eluent, IBMK, was found to be an important parameter among the variables of the on-line sorption system. It does influence the sensitivity in FI-FAAS, depending on the eluent of its divergence from the free uptake of nebulizer. The difference in the two flow-rates is an important feature of pump-propelled FI-FAAS system which invokes the possibility of independently optimizing the two parameters. Although optimum nebulization conditions always occur at relatively high uptake rates, the sample can be presented to the nebulizer at much lower flow-rates than the free uptake rate. In fact, this is an important measurement for improving the nebulization efficiency of the system [4, 82]. With a decrease of sample introduction rate from 6 to 0.1 ml/min, a nebulization efficiency of about 8% under the normal aspiration rate may be expected to increase to about 60% the decreased introduction rate [4].

Accordingly, the IBMK flow rate was set at 1.0 ml/min which was lower than the free uptake rate of nebulizer (4.5 ml/min). In addition, with lower flow rate, the consumption of IBMK was minimized.

3.2.8 Summary of the Optimum Conditions

The optimum conditions for the FI on-line sorption preconcentration of Cr(VI) for FAAS detection are summarized in Table 3.9.

Table 3.9 Optimum conditions for Cr(VI) determination

Parameters studied	Optimum conditions
Sample	Cr(VI) in 0.15 M HCl
Flow rate of sample	5.0 ml/min
Reagent	0.2% (w/v) APDC
Flow rate of reagent	4.0 ml/min
Eluent	isobutyl methyl ketone (IBMK)
Flow rate of eluent	1.0 ml/min
Length of KR	125 cm (PTFE 0.5 mm i.d.)
Preconcentration time	180 s

3.2.9 Oxidation of Cr(III) to Cr(VI)

The extraction of Cr(III) by the dithiocarbamate-IBMK system under the conditions usually employed for the extraction of Cr(VI) has been found to be difficult. The nonextractability of Cr(III) was ascribed to the difficulty of displacing the coordinated water from the strongly hydrated Cr(III) ion by the dithiocarbamate ligand [cited in 33]. Cr(VI) in contrast, reacts with APDC easily and quickly. The Cr (VI) is reduced to Cr(III) which forms two different complexes as shown in Fig. 3.14, bis[-pyrrolidine-1-dithioato-S,S']-[pyrrolidine-1-peroxydithioato-O,S]-Cr(III) and tris [pyrrolidine-1-dithioato-S,S']-Cr(III) [83]. Both complexes can be extracted into IBMK.

Harsh conditions were required for oxidation of Cr(III) to Cr(VI), as the dissociation of kinetically inert Cr(III) complexes was otherwise slow [77]. Cr(III) might also be present in organically bound species, which had to be converted into inorganic Cr by acid digestion [84].

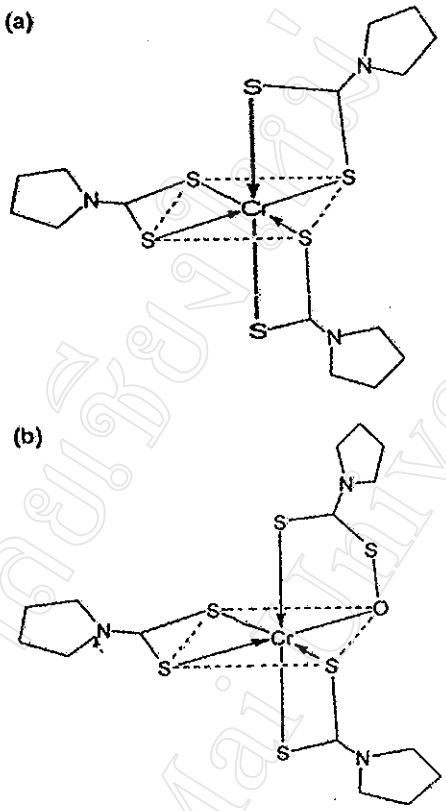

Figure 3.14 (a) tris[pyrrolidine-1-dithioato-S,S']-Cr(III) (b) bis[-pyrrolidine-1-dithioato-S,S']-[pyrrolidine-1-peroxydithioato-O,S]-Cr(III)

Trivalent Cr was more stable than hexavalent Cr; however, it could be oxidized easily to its hexavalent state using acidic permanganate or persulfate digestion. In alkaline solution, it had a much lower oxidation potential and it could be readily oxidized to chromate ion by aeration or by using hydrogen peroxide [86] and periodate [87] as oxidants.

The selection of the best oxidizing agent for Cr(III) was based on its ability to perform the oxidation rapidly and quantitatively, while not creating interferences in the analytical procedure and problems with the FIA paths. Oxidation

of Cr(III) to Cr(VI) with cerium (IV) sulfate as suggested by de Andrade *et al.* [88] was first considered, because this procedure could be performed on-line. However, Matsuoka *et al.* [85] suggested that, this oxidizing agents was not effective for the complete oxidation of Cr(III) when a large amount of organic compounds such as humic acid, which are oxidized together with Cr(III) by this oxidizing agent, was present; the Cr(VI) concentration in such a water sample was often observed to be higher than the total chromium concentration. For this reason, Ce(IV) is not so effective for the oxidation of Cr(III) in natural waters containing a large amount of organic compounds.

Gilbert and Clay [89] reported complete oxidation of Cr(III) in sea-water samples using permanganate; however, Beyermann [90] and de Jong and Brinkman [91] observed that oxidation of nanogram amounts of Cr(III) was not complete using this procedure. Miyazaki and Barnes [92] explained the incomplete recovery of Cr from sea-water with losses of chromyl chloride during the oxidation of Cr(III) to Cr(VI) with permanganate. Silver ion catalyzed peroxydisulphate, recommemded by Beyermann [93], was used successfully for the oxidation of Cr(III) [88]. This oxidation procedure was therefore studied in detail herein.

The rate of oxidation of Cr(III) to Cr(VI) in standard solutions was investigated. The relative oxidation yield was calculated, comparing the peak height values observed for identical concentration (0.1 mg/l) of Cr(VI) and the oxidized Cr (III), both measured under the same optimized conditions. The oxidation of Cr(III) by peroxydisulphate does not proceed well at room temperature. The oxidation rate could be accelerated by heating in a water bath at 80 ^{0}C [85]. The optimization of oxidation process was then studied at this temperature.

The effect of concentration of sulphuric acid was firstly studied for oxidation process. The results can be illustrated in Table 3.10 and Fig. 3.15.

Table 3.10 Effect of concentration of H_2SO_4 on Cr(III) oxidation

$[H_2SO_4]$ (M)	Peak height (cm)			Average (cm)	SD	Relative oxidation yield (%)
0.001	3.75	3.90	3.30	3.65	0.31	101.4
0.005	3.40	3.60	3.60	3.53	0.12	98.2
0.010	3.40	3.40	3.50	3.43	0.06	95.3
0.025	3.90	2.90	2.90	3.23	0.58	89.8

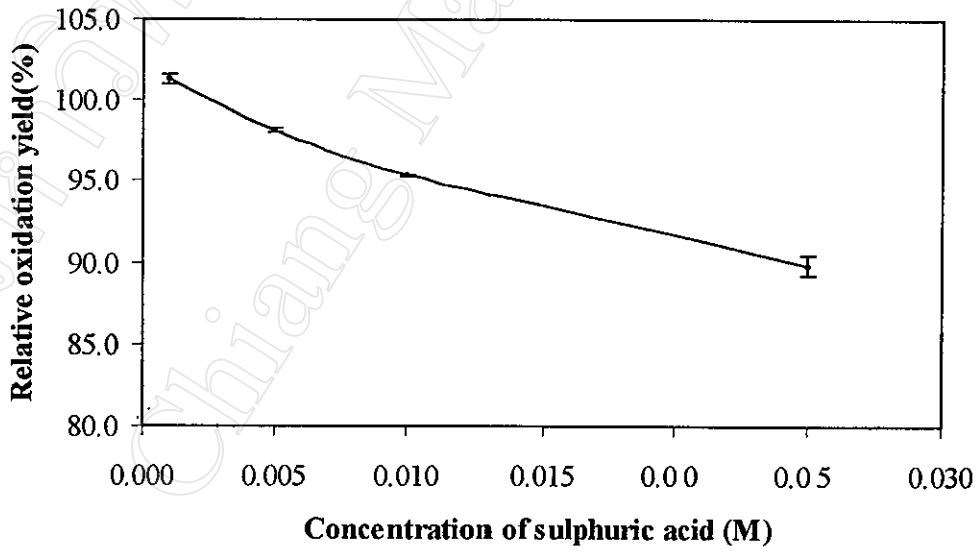

Figure 3.15 Effect of concentration of H_2SO_4 on the oxidation of 0.10 mg/l Cr(III) with 0.05 M $K_2S_2O_8$ at 80 ^{0}C for 30 min.

There was a marked influence of the sulphuric acid concentration in the Cr(III) solution on the oxidation yield, as indicated in Fig. 3.15. Possibly the Cr (III)-sulphate complexes that might be formed when Cr(III) is in sulphuric acid solution inhibit the oxidation reaction. In dilute solutions of sulphate and Cr(III) ion, the important chromium species is the monosulphatochromium (III) complex, present as an inert iner-sphere complex, $[Cr(H_2O)_xSO_4]^+$, and as a labile outer-sphere association (ion-pair) complex ion [93], $[Cr(H_2O)_6^{3+}SO_4^{2-}]^+$. The species $[Cr(SO_4)_2]^-$ appears when the sulphate ion concentration is increased [93]. The outer-sphere complexs of sulphate and hexaaquochromium (III) ion are in rapid equilibrium with their environment but the inner-sphere chromium sulphates are not. Although the rate of formation of these inner-sphere complexes is relatively slow [94], it may interfere when the Cr(III) is in a more concentrated sulphuric acid solution for some time. Therefore, the diluted sulphuric acid, 0.005 M, was applied in oxidation process.

The effect of peroxydisulfate concentration range from 0.0005-0.05 M on the oxidation yield was then examined. The results are depicted in Table 3.11 and Fig. 3.16.

As can be seen in Fig. 3.16, the maximum oxidation yield (98.7%) was observed when the concentration of peroxydisulphate was 0.001 M. This concentration was then used in oxidation process

Table 3.11 Effect of concentration of $K_2S_2O_8$ on Cr(III) oxidation

$[K_2S_2O_8]$ (M)	Peak height (cm)			Average (cm)	SD	Relative oxidation yield (%)
0.0005	2.10	2.10	2.00	2.07	0.06	88.7
0.0010	2.40	2.30	2.20	2.30	0.10	98.7
0.0025	2.10	2.05	1.90	2.02	0.10	86.6
0.0050	1.85	1.80	1.90	1.85	0.05	79.4
0.0100	1.60	1.40	1.30	1.43	0.15	61.5
0.0500	0.65	0.50	0.50	0.55	0.09	23.6

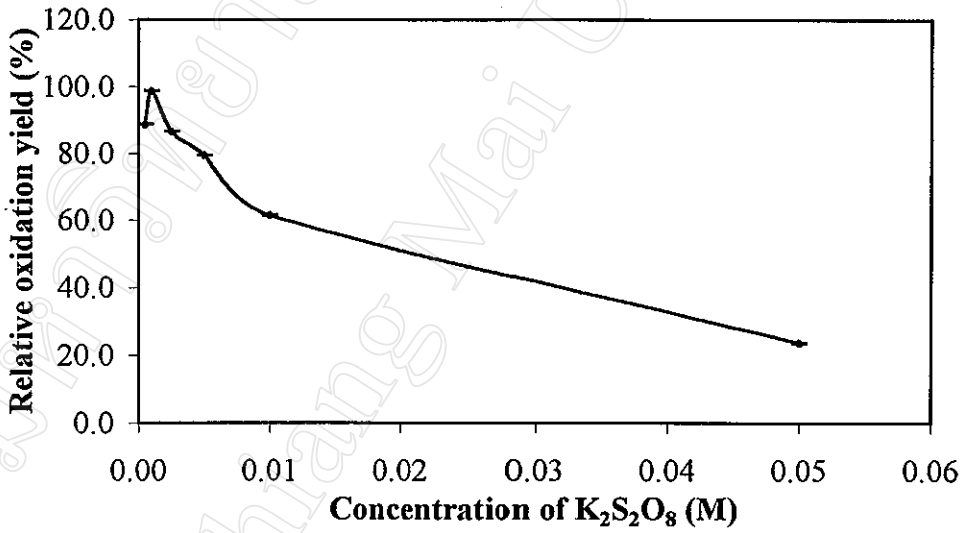

Figure 3.16 Effect of concentration of $K_2S_2O_8$ on the oxidation of 0.10 mg/l Cr(III) in 0.005 M H_2SO_4 at 80 ^{0}C for 30 min.

Quantitative oxidation was further studied by varying the heating time from 10 to 60 minutes. The results are exhibited in Table 3.12 and Fig. 3.17.

Table 3.12 Effect of oxidation time on Cr(III) oxidation

Time for oxidation (min)	Peak height (cm)			Average (cm)	SD	Relative oxidation yield (%)
10	4.80	4.50	4.60	4.63	0.15	79.9
20	5.70	6.00	6.00	5.90	0.17	101.7
30	6.00	6.00	6.20	6.07	0.12	104.6
40	6.10	6.40	5.80	6.10	0.30	105.1
50	6.10	6.20	6.10	6.13	0.06	105.7
60	6.30	5.60	6.30	6.07	0.40	104.6

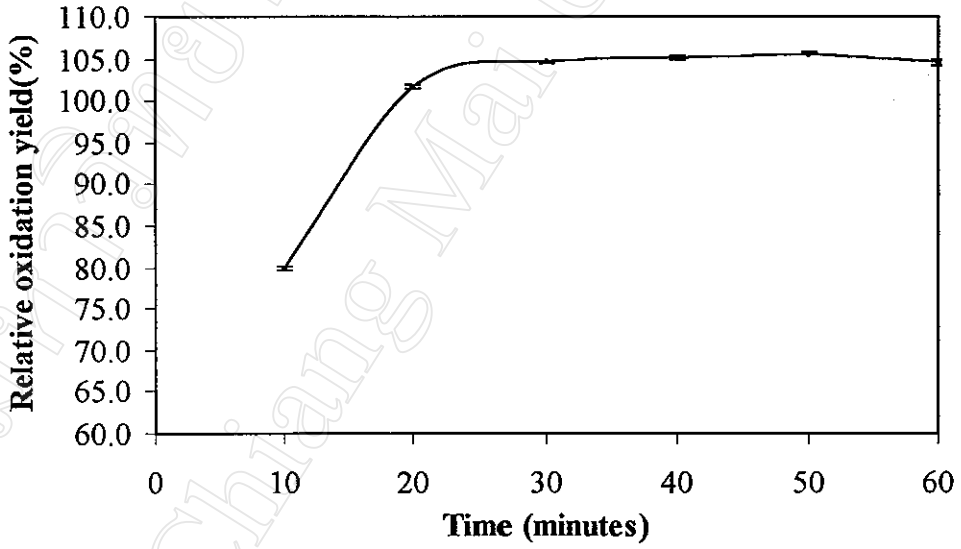

Figure 3.17 Effect of oxidation time on the oxidation of 0.10 mg/l Cr(III) in 0.005 M H_2SO_4 with 0.001 M $K_2S_2O_8$ at 80 ^{0}C.

As accomplished in Fig. 3.17, the 0.1 mg/l Cr(III) standard solution could be quantitatively oxidized to Cr(VI) after heating for at least 20 minutes at 80 ^{0}C. However, it was found to be more difficult to oxidize Cr(III) in mineral water to

Cr(VI). It could be oxidized completely to Cr(VI) after heating for 30 minutes. This means that the rate of oxidation was dependent on the heating conditions and the matrix composition. Therefore, the 30 minutes for heating was used for successfully oxidation of Cr(III) to Cr(VI).

The influence of varying concentration ratios of Cr(III) in Cr(VI) for quantitative oxidation of Cr(III) was shown in Table 3.13. From this table, it was clear that at any concentrations of Cr(III) in the presence of Cr(VI) was not interfere in the oxidation yield. The optimized condition used for Cr(III) oxidation was therefore successfully applied for Cr(VI) determination in any real samples.

Table 3.13 Relative oxidation yield of standard mixtures of Cr(III) and Cr(VI)

Chromium mixtures (mg/l) Cr(III) : Cr(VI)	**Relative oxidation yield (%)**
0.00 : 0.10	104.6
0.02 : 0.08	101.4
0.04 : 0.06	107.5
0.05 : 0.05	98.6
0.06 : 0.04	98.7
0.08 : 0.02	104.6
0.10 : 0.00	101.4

3.2.10 Evaluation of Potential Interferences for Cr(VI)

APDC forms complexes with most transition metals but does not form complexes with alkaline, alkaline earth and rare earth metals [33, 63]. In this way, the determination of Cr(VI) in real samples is affected only by some other transition metals (see Table 3.14). The tolerance to interferences at maximum possible

concentration levels were not good without using any masking agents especially for Cu(II) and Cd(II). Different masking agents, EDTA, hydroxyquinoline, KSCN, thiourea, ascorbic acid and tetracyclin, were studied to overcome the interfering effects. The 0.4% (w/v) EDTA was found to be effective for all interference studied. At effective concentration of EDTA in the sample solution, the masking agent had no deleterious effects on the preconcentration of the analyte, therefore addition of the masking agents to standard solutions was not required.

The effects of interfering ions were studied by adding various ions to standard solutions of 0.05 mg/l Cr(VI). The effect was expressed as recovery for the levels added. The results are shown in Table 3.14 and summarized in Table 3.15.

3.2.11 Analytical Performance of the FI On-line Sorption Preconcentration of Cr(VI) on KR

Several parameters important for quantitative analysis of Cr(VI), including linearity, limit of detection and reproducibility, were examined under the above optimized conditions. A linear relationship between peak height and concentration of Cr(VI) was studied in the 0.01-0.40 mg/l Cr(VI) range for preconcentration time of 180 s with 125 cm KR tubing length. The results are shown in Table 3.16 and Fig. 3.18. The peak height increased linearly up to 0.20 mg/l, leveling off with further increased in Cr(VI) concentrations. The linearity range was therefore existed within the interval of 0.01-0.20 mg/l. An example of the peak height signal and the linear calibration curve for determination of Cr(VI) are shown in Fig. 3.19 and 3.20, respectively.

Table 3.14 Effect of interference study for 0.05 mg/l Cr(VI)

Interference	Concentration added (mg/l)	Recovery (%)
Cu(II)	0.1	95.2
	0.2	77.4
	0.3	58.3
Cd(II)	0.1	103.6
	0.2	108.3
	0.3	121.4
Ni(II)	0.1	104.2
	0.2	105.9
	0.3	105.1
	0.4	105.1
	0.5	114.1
	0.6	129.0
Zn(II)	1.5	99.4
	1.6	98.8
	1.7	101.3
	1.8	103.0
	1.9	124.9
	2.0	130.9
Co(II)	0.1	101.2
	0.2	98.3
	0.3	78.9
Pb(II)	0.1	95.1
	0.2	103.8
	0.3	93.9
	0.4	67.8
Fe(III)	0.5	101.9
	0.6	103.8
	0.7	94.4
	0.8	98.8
	0.9	96.6
	1.0	87.6
Mn(II)	1.5	100.9
	2.0	110.5
	2.1	114.3
	2.2	127.6

Table 3.15 Summary of the tolerance limit of the interferent effects on the determination of 0.05 mg/l Cr(VI)

Interference	Tolerance concentration*(mg/l)
Cu(II)	0.1
Cd(II)	0.2
Co(II)	0.2
Pb(II)	0.3
Ni(II)	0.4
Fe(III)	0.9
Zn(II)	1.8
Mn(II)	2.0

*The concentration of an ion was considered to be interfering when causing the percentage of recovery of more than ±10% with respect to the recovery of Cr(VI) alone.

Table 3.16 Relationship between peak height and concentration of Cr(VI)

[Cr(VI)] (mg/l)	Peak height (cm)			Average (cm)	SD
0.010	0.35	0.33	0.37	0.35	0.020
0.025	0.90	0.88	0.93	0.90	0.025
0.050	1.45	1.30	1.45	1.40	0.087
0.075	1.60	1.80	1.70	1.70	0.100
0.100	2.45	2.40	2.35	2.40	0.100
0.200	4.40	4.20	4.40	4.33	0.115
0.300	4.80	4.75	5.00	4.85	0.132
0.400	5.40	5.35	5.40	5.38	0.029

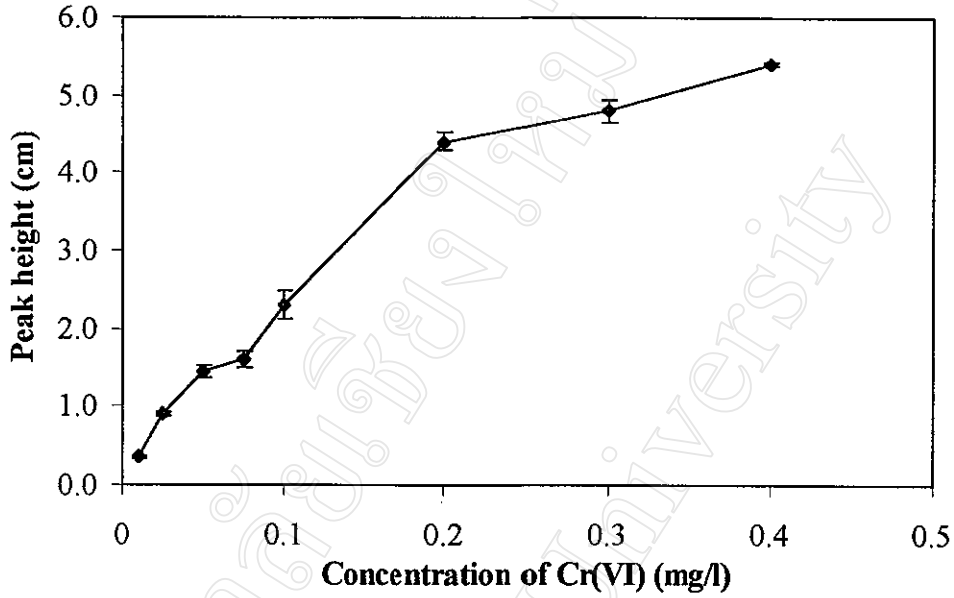

Figure 3.18 Relationship between peak height and concentration of Cr(VI)

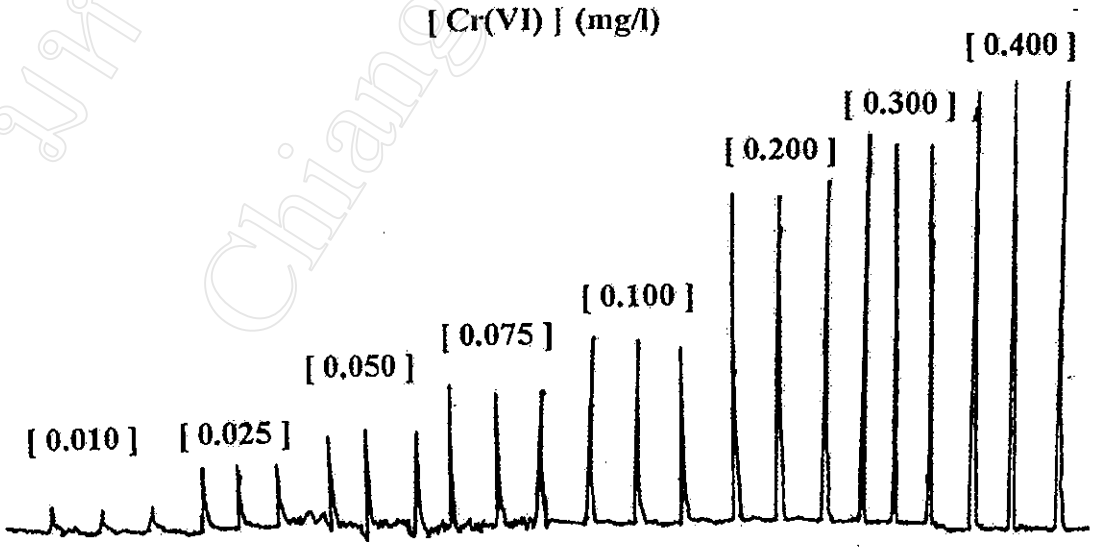

Figure 3.19 The peak height obtained from the recorder

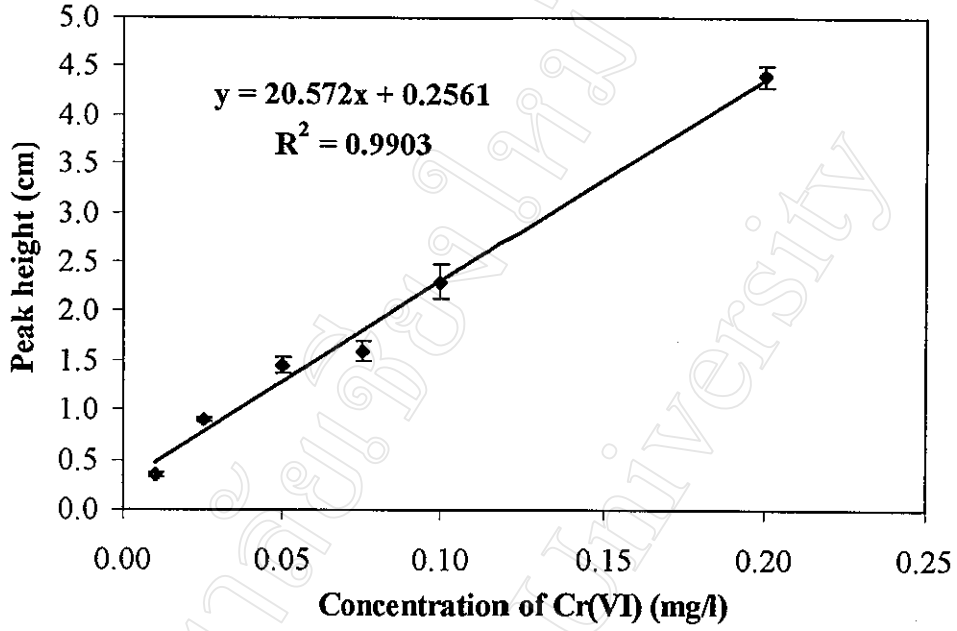

Figure 3.20 Calibration curve of Cr(VI)

A definition of detection limit in this work is based on the analyte concentration which gives the response signal 3 times that of the standard deviation of the blank plus response signal [95]. The detection limit for Cr(VI) was found to be 0.004 mg/l under the optimized conditions as shown in Table 3.17.

Table 3.17 Signal of reagent blank

Blank signal (cm)	SD	3*SD	Regression equation of calibration curve	Detection limit (mg/l)
0.90, 0.95, 1.00, 1.10, 1.00, 0.95, 0.90, 0.95, 0.95, 0.95, 0.95	0.055	0.166	Y = 20.629x + 0.2434	0.004

The repeatability of the system was examined by making eleven consecutive runs with Cr(VI) concentrations of 0.025 mg/l and 0.10 mg/l. The repeatability of the method can be evaluated from the standard deviation (SD) and the percentage of relative standard deviation (%RSD). The results are shown in Table 3.18.

Table 3.18 Repeatability for Cr(VI) determination

Concentration of Cr(VI) (mg/l)	Peak height (cm)	Average	S.D.	%RSD
0.025	1.85, 1.80, 1.80, 1.75, 1.75, 1.75, 185, 1.70, 1.70, 1.70, 1.75	1.76	0.06	3.13
0.100	2.40, 2.45, 2.45, 2.45, 2.55, 2.40, 2.40, 2.35, 2.40, 2.40, 2.40	2.42	0.05	2.14

An enrichment factor (EF) and the retention efficiency were calculated from the ratio of the slope of the calibration curves with and without a preconcentration step, respectively. Without preconcentration, 2.0 ml of a Cr(VI) solution was introduced directly into the FAAS. With preconcentration, sample solution was loaded on the appropriate reactor (KR) with a loading time of 180 s, the enrichment factor and retention efficiency of 93.3 and 11.9% were obtained respectively, allowing a sample frequency of 16 samples/h. A concentration efficiency (CE) of 24.9 was then obtained.

Characteristic data for the performance of the on-line sorption preconcentration system for Cr(VI) is summarized in Table 3.19.

Table 3.19 Performance of the FI on-line sorption preconcentration of Cr(VI) for FAAS detection

Parameters studied	Analytical Characteristic
Sample flow rate (ml/min)	5
Calibration range (mg/l)	0.01-0.20
Regression equation (six standard, n=3, [Cr] (mg/l))	20.629[Cr]+0.2434 (r^2=0.9918)
Sampling frequency (*f*) (sample/h)	16
Relative standard deviation (%) (n=11; 0.025 and 0.10 mg/l, respectively)	3.13, 2.14
Limit of detection (3σ) (mg/l)	0.004
Enrichment factor (EF)	93.3
Concentration efficiency (CE = EF*f/60)	24.9
Retention efficiency (%)	11.9

3.2.12 The Determination of Cr(VI) and Total Chromium in Different Water Samples

The accuracy of the method was firstly checked by analyzing a SRM NIST-1640, trace elements in natural water. The results are shown in Table 3.20.

Table 3.20 Analysis of reference materials

Sample	Certified value (mg/l)			Amount found[a] (mg/l)		
	Total Cr	Cr(VI)	Cr(III)	Total Cr	Cr(VI)	Cr(III)
NIST-1640	0.025	-	0.025	0.028±0.003	nd[b]	0.028±0.003
NIST-1640 (spiked with Cr(VI))	0.050	0.025	0.025	0.053±0.003	0.027±0.008	0.026±0.009

[a]Mean ± SD (n = 3)

[b]nd = not detected

The Cr(VI) was determined directly by the developed preconcentration method. Total chromium was determined after oxidation of Cr(III) to Cr(VI) by potassium peroxydisulphate. Chromium (III) was then calculated by the difference between total Cr concentration and that of Cr(VI).

The certified Cr-content was stated to be 38.6±1.6 µg/l. Before analysis the reference standard was diluted until a concentration of 0.025 mg/l of Cr was obtained. After analyzing this SRM, Cr(VI) content was not detected. The explanation for this might either be due to the fact that all Cr originally present was as in the state of Cr(III) or that any initially Cr(VI) present in the SRM was below the detection limit or it had been reduced to Cr(III) which was more stable than Cr(VI).

The most challenging problem determining traces of Cr(VI) is the preservation of its oxidation states. Conventionally, dilute nitric acid is used to preserve natural samples in order to prevent the adsorption of trace elements in solution on to the walls of the container, and this is also the case in this instance, where NIST-1640 has been preserved in 0.5 M HNO_3. Cr(VI) exists predominantly as $HCrO_4^-$ in acidic solution which is a strong oxidizer. It can be easily reduced to Cr(III) in the presence of organic matter [96-98]. At pH >6.5 Cr(VI) exists predominantly as CrO_4^{2-}, which is less reactive than $HCrO_4^-$. Therefore, as recommended by Sperling *et al.* [77], the use of nitric acid for sample preservation should be strongly discouraged, at least when speciation of Cr is wanted. Rather, good stabilization condition of both Cr(III) and Cr(VI) is obtained by affixing the pH at 6.4 with HCO_3^- /H_2CO_3 buffer under a CO_2 blanket which will prevent Cr(VI) reduction [99-104].

With the NIST standard sample being stabilized with 0.5 M nitric acid, the Cr-content, therefore, is very likely exclusively Cr(III). For this reason, no Cr(VI)

content was found in the NIST-1640. After Cr(III) was oxidized to Cr(VI), the result agreed well with the certified value (0.025 mg/l) indicating that the present procedure could reliably be used for the analysis of total chromium in natural water.

The accuracy for the determination of Cr(VI) was checked by spiking the standard with 0.025 mg/l of Cr(VI) into the reference standard water sample (NIST-1640) containing 0.025 mg/l of Cr(III) of NIST-1640 resulting in the concentration of total chromium of 0.050 mg/l. As can be seen from Table 3.20, that a reasonable recovery of 0.027 mg/l of Cr(VI) and 0.053 mg/l of total chromium were found. After subtraction the amount of total chromium with that of Cr(VI), the amount 0.026 mg/l of Cr(III) was obtained which was in good agreement with the certified value (0.025 mg/l).

Using the proposed sorption and preconcentration procedure, the Cr (VI) and total chromium contents in various water samples were further determined. The Cr contents measured are summarized in Table 3.21.

It was seen that both Cr(VI) and total Cr in all water samples of interest were not detected in every sample tested. This indicated that the Cr contents were below the detection limit of this procedure. Since the Maximum Contaminant Level (MCL) of total chromium for the primary drinking water standards of EPA is set at 0.10 mg/l [105], therefore, the concentration of 0.025 mg/l of each Cr(VI) and Cr(III) was added into each samples in order to evaluate the performance of the developed system. A reasonable recovery of the amounts added were found for all samples, which demonstrated the satisfactory performance and selectivity of the proposed procedure.

Table 3.21 Determination of Cr(VI) and total Cr in various water samples

Sample	Amount added (mg/l)			Amount found (mg/l)[a]		
	Total Cr	Cr(VI)	Cr(III)	Total Cr	Cr(VI)	Cr(III)
Drinking water	-	-	-	nd[b]	nd	nd
(Singha)	0.050	0.025	0.025	0.047±0.004	0.027±0.003	0.020±0.005
Mineral water	-	-	-	nd	nd	nd
(Mont Fleur)	0.050	0.025	0.025	0.052±0.004	0.021±0.004	0.031±0.006
Mineral water	-	-	-	nd	nd	nd
(Whistler)	0.050	0.025	0.025	0.049±0.006	0.029±0.006	0.020±0.008
Mineral water	-	-	-	nd	nd	nd
(Aura)	0.050	0.025	0.025	0.049±0.006	0.027±0.005	0.022±0.007
Tap water I	-	-	-	nd	nd	nd
	0.050	0.025	0.025	0.042±0.009	0.028±0.005	0.014±0.010
Tap water II	-	-	-	nd	nd	nd
	0.050	0.025	0.025	0.041±0.009	0.030±0.008	0.011±0.012

[a]Mean ± SD (n = 3).
[b]nd = not detected

3.3 FI On-line Preconcentration of Low Levels of Cr(VI) with Detection by ETAAS. Comparison of Using an Open Tubular PTFE Knotted Reactor and a Column Reactor Packed with PTFE Beads

Since 1994, the knotted reactor (KR) has been extensively employed for the FI on-line preconcentration system via molecular sorption of neutral metal complexes onto its interior surface as a result of its many advantages over the other sorbent material. Although the open-ended nature of the KR entails the clear advantage of a

low hydrodynamic impedance and allows high sample loading flow rates for obtaining the better enrichment factors, the low retention efficiency on the inner wall of the KR for most metal complexes, however, restricts the significant improvement of its preconcentration capability. It might be due to the fact that the adsorption efficiency depends on the possibility of the non-charged complexes formed to become effectively sorbed and retained on the wall. The reported values of retention efficiency are generally within the range of 30-60% [54], while some are even lower than 20%, e.g., by using 8-HQ as complexing agent [59]. In addition only 11.9% of the retention efficiency was gained for the FI on-line sorption preconcentration of Cr (VI) in the previous work (Section 3.2).

The statistical probability for adsorption and retention of non-charged chelate species onto the surface of the PTFE surface might be expected to become improved if the diffusion/convection distances to be traveled by the analyte complex were to be minimized. Therefore, it might be judicious to replace the Teflon KR by a column reactor packed with small PTFE beads [106, 107]. This would be potentially entail the feasibility of attaining a larger, effective hydrophobic surface area. The beneficial use of a packed column reactor was actually indicated most recently by Anthemidis *et. al.* [108, 109]. They used a column filled with PTFE turnings for on-line preconcentration of Cu(II) and Cr(VI) via complexation with ammonium pyrrolidinedithiocarbmate (APDC) and elution by IBMK followed by detection by flame AAS. However, not only is it difficult to prepare such columns reproducibly, but the active surface area per unit weight of PTFE is also much lower than that of small Teflon beads, which therefore makes these ones preferable both in terms of effectiveness and in simplicity of operation.

The aim of this present section was, therefore, to demonstrate the efficiency of using an incorporated column reactor packed with small Teflon beads for appropriate preconcentration of non-charged metal complexes. With respect to the determination of Cr(VI) via complexation with APDC, elution by ethanol and ensuing detection by ETAAS, its performance is compared to that of an open Teflon tubular KR of similar internal surface area.

Establishment of experimental parameters for optimization was initiated by finding the optimum length of the KR for the on-line preconcentration of Cr(VI). The PTFE beads packed column which offered a total surface area corresponding to the inner surface area of KR at optimum length was then prepared. The results obtained from both the KR and the packed column reactor at the same optimum conditions are compared and discussed in the following sections.

3.3.1 Manifold Design and Operational Sequences

For the coupling of FI on-line sorption preconcentration to ETAAS, the necessary manipulatory operations includes (a) effective entrapment of analyte in the preconcentration unit; (b) washing of the preconcentration unit to remove some possible interfering matrix components; (c) quantitative elution in the smallest possible volume of eluent; (d) reproducible transport of the concentrate to the ETAAS with minimum dispersion; and (e) efficient cleansing of the entire system to avoid carry-over between individual samples.

The washing step before elution, which is unimportant and usually omitted in FAAS determinations, is generally accepted as indispensable (excluding samples with very low matrix contents) for ETAAS, where matrix interferences are

much more serious [110]. Therefore, to prevent carry-over from the sample line, a wash solution should be administered, i.e. directed through the pertinent part of the sample conduit in between sample runs.

When using ETAAS as the detector, quantitative dissolution of the retained analyte in the smallest possible volume of eluent is important to satisfy the restricted volumetric requirements of the graphite tube/platform. Therefore, the FI-elution techniques is especially crucial when designing the optimal FI-ETAAS system. The FI-elution technique considered were time-based zone sampling, and momosegmentation of the concentrate by previous entrapment of the eluent by means of air, respectively. However, the former approach, which has been reported by Sperling [77, 111] and Fang [112], was found to be less desirable. Although zone sampling technique in ETAAS permits the introduction of any portion of the concentrate without deterioration of reproducibility as long as the total mass injected remains constant [113], the method includes two extra experimental parameters to be optimized and controlled. They are, the zone-sampling time and, particularly, the eluent flow rate during zone sampling which might be difficult to maintain constant over longer periods of times of operation.

In order to adapt the final eluate volume to that required for introduction into a graphite furnace, during elution an eluent loop was employed to introduce a fix small volume of eluent, and an air flow was used to drive the eluent into the eluate delivery tube which was then introduced into the ETAAS where the resulting absorbance as peak area was measured [114, 115]. Beinrohr *et al.* [116] were the first who used an air transportation system for elution in column preconcentration for ETAAS. However, the performance was limited by the quality of

the air drive, which was an air-flow provided by the spectrometer gas supply. In later applications, peristaltic pumps were used to provide air flows which were better controlled. A significant reduction of dispersion at the elution and eluate introduction stages was achieved when the controlled air flow was used [55].

With all above considerations, the FI manifold and the operation sequences used in this work for the preconcentration of Cr(VI) with an ETAAS detection was, therefore, designed and fabricated as illustrated in Fig. 2.3 and Table 2.5, respectively. The proposed FI-system satisfies all the necessary manipulatory operations needed on-line, thereby allowing to achieve the highest possible sensitivity.

3.3.2 Optimization of the Graphite Furnace Temperature Program

The pyrolysis curve for Cr(VI)-PDC complex originally in ethanolic solution is shown in Table 3.22 and Fig. 3.21. The integrated absorbance was the highest at a pyrolysis temperature of 1100 ^{0}C. At higher temperatures, the integrated absorbance decreased, indicating that the thermal stability of the Cr(VI)-PDC originally in ethanol was essentially the same as that of Cr(VI) originally in aqueous solution [77].

The atomization curve for Cr(VI)-PDC complex is exhibited in Table 3.23 and Fig. 3.22. The results revealed that the integrated absorbance increased with the atomization temperature within the range of 2,200-2,400 ^{0}C, and reached a maximum at 2,400 ^{0}C. When the atomization temperature exceeded 2,400 ^{0}C, the signal decreased with increasing temperature.

From the above results, the graphite furnace temperature program for the determination of Cr(VI)-PDC complex in ethanolic solution was set under the optimum conditions as shown in Table 3.24.

Table 3.22 Effect of pyrolysis temperature on the determination of Cr(VI)-PDC complex

Pyrolysis temperature (^{0}C)	Integrated absorbance			Average	SD
1100	0.274	0.282	0.275	0.277	0.004
1200	0.202	0.184	0.192	0.193	0.009
1300	0.167	0.172	0.170	0.170	0.003
1400	0.187	0.189	0.188	0.188	0.001
1500	0.182	0.178	0.181	0.180	0.002
1600	0.159	0.162	0.163	0.161	0.002

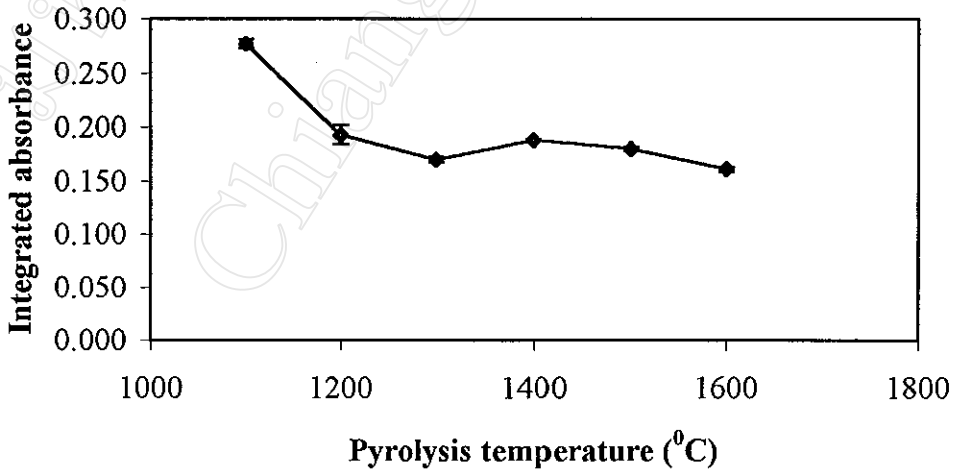

Figure 3.21 Effect of pyrolysis temperature on the signal of Cr(VI)-PDC complex in ethanolic solution (atomization temperature was set at 2300 ^{0}C)

Table 3.23 Effect of atomization temperature on the determination of Cr(VI)-PDC complex

Atomization temperature (^{0}C)	Integrated absorbance			Average	SD
2200	0.123	0.120	0.118	0.120	0.003
2300	0.143	0.142	0.144	0.143	0.002
2350	0.140	0.146	0.143	0.143	0.007
2400	0.152	0.158	0.156	0.155	0.008
2450	0.141	0.140	0.142	0.141	0.005
2500	0.151	0.140	0.148	0.146	0.006

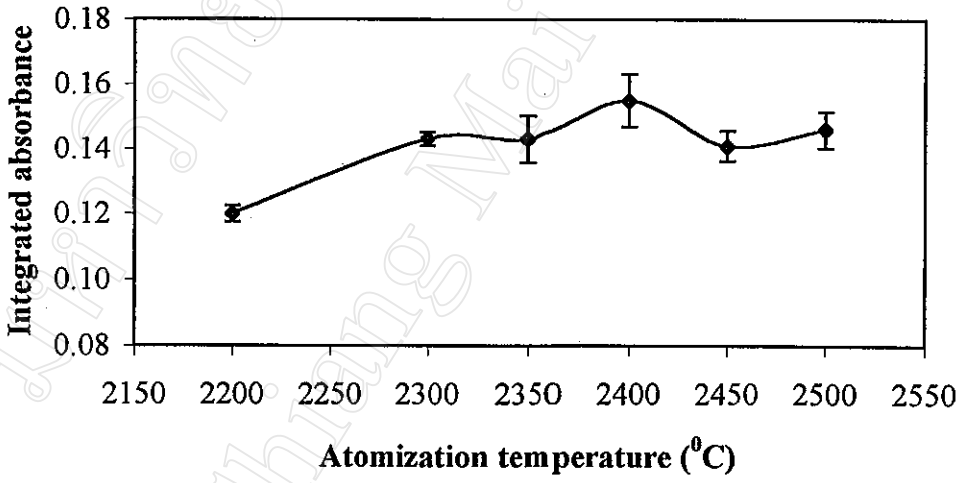

Figure 3.22 Effect of atomization temperature on the signal of Cr(VI)-PDC complex in ethanolic solution (pyrolysis temperature was set at 1100 ^{0}C)

Table 3.24 Graphite furnace temperature program for the determination of Cr(VI) in the ethanolic using pyrolytically coated graphite tubes with the platform

Step	Temperature (^{0}C)	Ramp (s)	Hold (s)	Ar flow rate (ml/min)
1	60	5	20	300
2	90	5	20	300
3	120	5	25	300
4	1100	5	25	300
5	2400	0	5	0
6	2700	1	3	300

3.3.3 Optimization of the Sample Acidity, [HCl], the Concentration of Complexing Agent, [APDC], and the Concentration of the Washing Solution, [WS]

In order to limit the number of experimental factors, a variable-size simplex approach was employed for optimization of the starting conditions for the preconcentration procedure. The three critical variables for the formation of the Cr (VI)-PDC complex and its adsorption on the inner wall of the KR were considered. These are the sample acidity, [HCl], the concentration of the chelating agent, [APDC], and the concentration of the washing solution (diluted APDC), [WS]. In this work, HCl was more preferable than HNO_3 and H_2SO_4 (see Section 3.2.3), and hence was selected to adjust the sample acidity. Regarding to the APDC, apart from its tendency of forming strong metal complexes, this chelating agent also provides the advantage of being readily soluble in water and exhibiting good stability in acidic medium [117].

A washing period of 10 s at a flow rate of 3.0 ml/min was affixed in the optimization process. The [HCl], [APDC] and [WS] were studied in the range of 0.005-0.03 M, 0.05-0.3% (w/v) and 0.005-0.03% (w/v), respectively. The relationship between the vertex number and the response signal is illustrated in Fig. 3.23. At the vertex number of 7, the highest response was gained. From this result, the optimum conditions were found to be 0.015 M for HCl, 0.17% (w/v) for APDC and 0.015% (w/v) for WS. These conditions were employed in the further optimization steps.

Figure 3.23 The relationship between the vertex numbers and response signals of Cr(VI)

3.3.4 Optimization of the Sample and the APDC Flow Rates

An effective preconcentration and formation of the Cr(VI)-PDC complex was influenced both by the flow rate of the sample and that of APDC. A flow rate ratio of the sample and the APDC was therefore investigated. The flow rates of the sample and the APDC were varied from 0.51-3.53 ml/min and 0.30-2.40 ml/min, respectively. The results are shown in Table 3.25 and Fig. 3.24. They

revealed that the integrated absorbance was almost constant at a sample/APDC flow rate ratio in the range of 1.3-1.7. In order to obtain the highest sensitivity, the highest sample loading flow rate of 5.0 ml/min was chosen. For keeping a sample/APDC flow rate ratio in the optimum interval of 1.3-1.7, an APDC flow rate of 3.0 ml/min was adopted.

Table 3.25 Effect of sample and APDC flow rate ratio on the determination of Cr(VI)-PDC complex

Sample/APDC flow rate ratio	Integrated absorbance			Average	SD
1.22	0.202	0.205	0.204	0.204	0.001
1.30	0.358	0.339	0.349	0.349	0.009
1.54	0.386	0.376	0.381	0.381	0.005
1.67	0.393	0.368	0.381	0.381	0.012
2.00	0.279	0.306	0.293	0.293	0.014

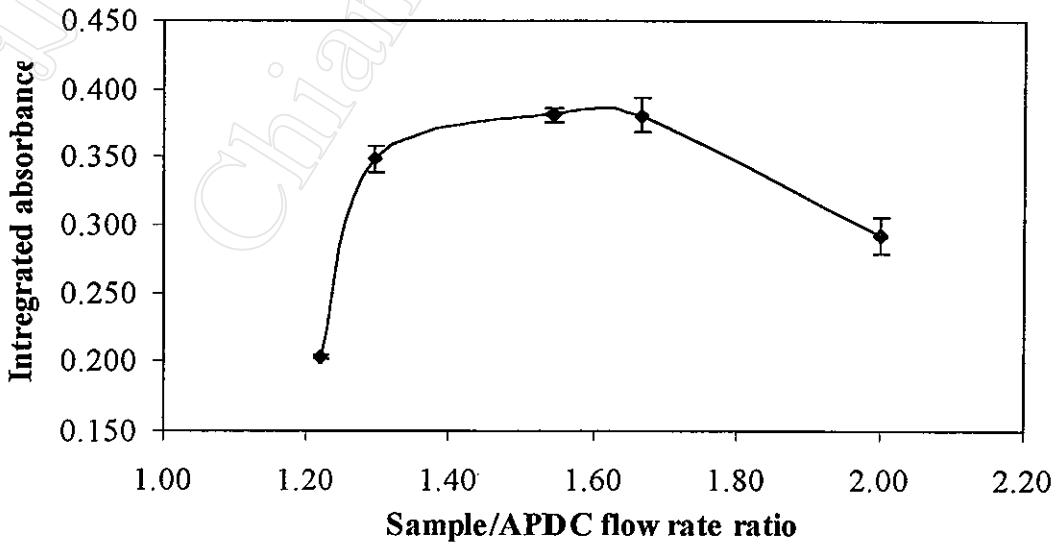

Figure 3.24 Effect of the sample and the APDC flow rate ratio on the preconcentration of 1.0 μg/l Cr(VI) in the KR (L_{KR} = 125 cm) for a preconcentration period of 60 s

3.3.5 Optimization of the KR Tubing Length

The influence of the length of the PTFE KR on the preconcentration of Cr(VI) was investigated in the range of 50-200 cm for a fixed preconcentration time period of 60 s. The results are shown in Table 3.26 and Fig. 3.25. As can be seen in Fig. 3.25, the integrated absorbance was found to increase linearly with increasing KR tubing length up to 125 cm. At longer tubing length, the signal remained constant because the flow impedance started to influence the mixing of the reaction media and thereby the adsorption of the complex. Therefore, a KR with a tubing length of 125 cm was selected in the following experiments.

Table 3.26 Effect of the KR length on the determination of Cr(VI)-PDC complex

KR length (cm)	Integrated absorbance			Average	SD
50	0.158	0.153	0.147	0.153	0.006
75	0.170	0.189	0.175	0.178	0.010
100	0.197	0.195	0.212	0.201	0.009
125	0.226	0.221	0.209	0.219	0.009
150	0.216	0.219	0.219	0.218	0.002
200	0.227	0.237	0.204	0.223	0.016

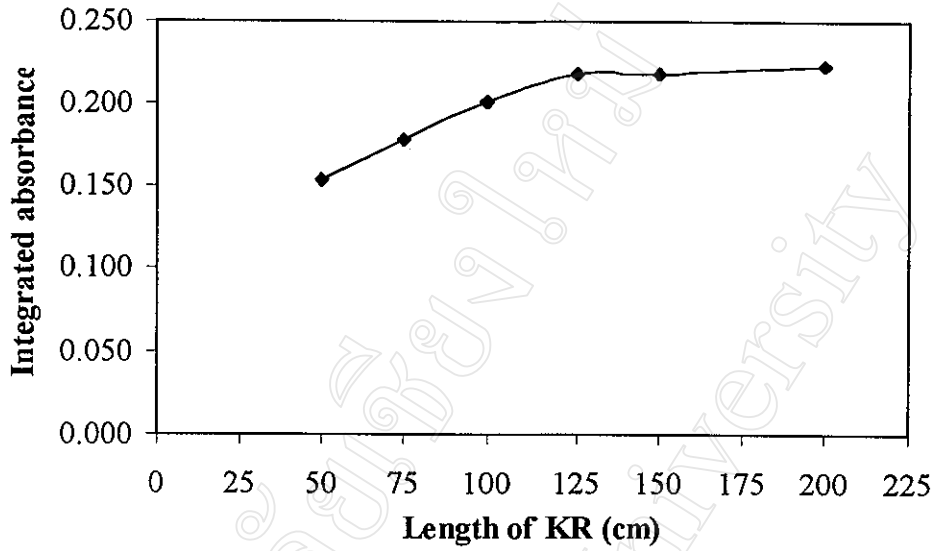

Figure 3.25 Effect of the length of the KR on the preconcentration of 1.0 μg/l Cr(VI) for a preconcentration time of 60 s

3.3.6 Optimization of the Sample Loading Time

The influence of sample loading time was studied in the range from 30 to 180 s. The results are illustrated in Table 3.27 and Fig. 3.26. As it appears from the results depicted in Fig. 3.25, the adsorption increased linearly up to 150 s and remained practically constant above this value and up to 180 s. This was probably due to a relatively high saturation of APDC on the inner wall of the KR, where the agent was present in large excess. Thus, a 60 s loading time was chosen as a compromise between medium sample consumption, sufficient sensitivity and resonable sampling frequency.

Table 3.27 Effect of sample loading time on the determination of Cr(VI)-PDC complex

Sample loading time(s)	Integrated absorbance			Average	SD
30	0.251	0.247	0.234	0.244	0.009
60	0.353	0.342	0.336	0.344	0.009
90	0.489	0.432	0.469	0.463	0.015
120	0.541	0.572	0.555	0.556	0.016
150	0.646	0.660	0.629	0.645	0.016
180	0.667	0.643	0.656	0.655	0.012

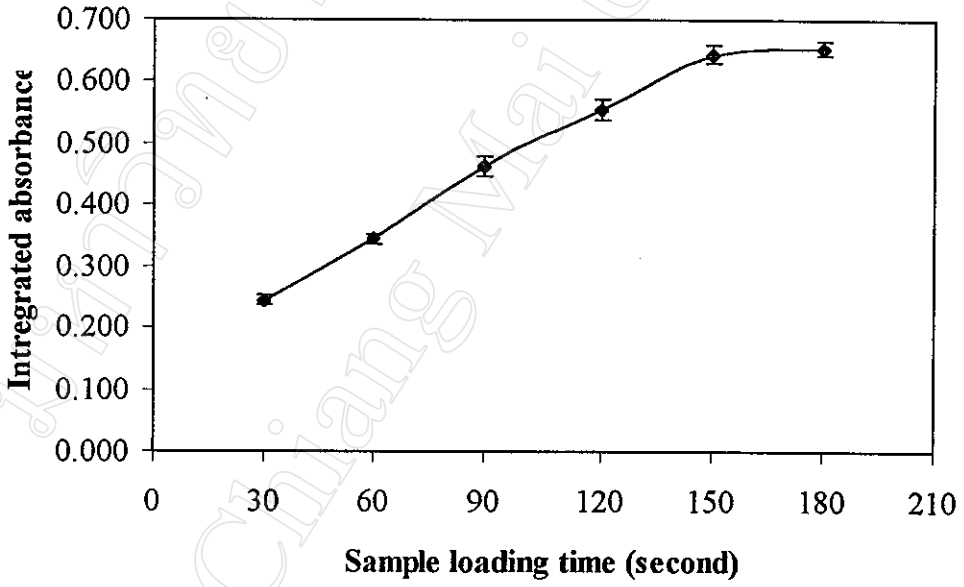

Figure 3.26 Effect of sample loading time on the preconcentration of 1.0 μg/l Cr(VI) in the KR of 125 cm

3.3.7 Optimization of the Experimental Parameters of the Elution and the Ensuing Introduction into the ETAAS

The choice of a suitable eluent is important for the analytical performance of an FI on-line preconcentration system. In this work, ethanol was selected as the most suitable eluent for the proposed FI preconcentration and quantitation of Cr(VI) with ETAAS detection not only because it exhibits a large concentration distribution ratio for Me-PDC complexes, but also because it has high volatility and yields low background. Mono-segmentation by means of air was utilized for transportation of the eluate. Quantitative elution of the analyte was achieved by using a segment of 35 μl of absolute ethanol, which satisfied the restricted volumetric requirements of the graphite platform. The flow rate used for the elution was varied in the range 0.6-1.5 ml/min. A flow rate at the lower end of this range was found preferable in the ensuing work, because the slower eluent flow favored both the recovery of the sorbed analyte from the inner walls of the KR and the accommodation of the eluate in the graphite tube. Using this flow rate, an 85 s elution time was needed for the complete transfer of the eluent from the eluent loop through the KR and the delivery tube to the ETAAS.

3.3.8 Comparative Preconcentration and Determination of Cr(VI) by On-line Sorption on KR and a Column Reactor Packed with PTFE Beads

Based on the optimum conditions found in Section 3.3.5, a PTFE bead packed column reactor with a length of 1.5 cm and loaded with 72 mg of PTFE beads (100 μm) was made. This reactor had a total surface area corresponding to the inner

surface area of the 125 cm (i.d. 0.50 mm) long KR (see Appendix B). The analytical performance of the KR and the packed column under identical optimum conditions, as described earlier in Sections 3.3.3-3.3.7, were investigated. A linear relationship between the integrated absorbance and concentration of Cr(VI) was studied over the ranges of 0.005-1.500 μg/l and 0.005-1.250 μg/l for the preconcentration system using the KR and the PTFE beads packed column, respectively. The calibration curves were linear within the 0.01-1.25 μg/l and 0.005-1.00 μg/l Cr(VI) ranges for the KR and packed column system, respectively. The results are shown in Tables 3.28-3.29 and Fig. 3.27-3.28. The regression equations for the calibration graphs using the KR and the PTFE beads packed column are $y=0.3669X+0.0096$ ($r^2=0.9992$) and $y=0.6776X-0.0009$ ($r^2=0.9955$), respectively.

Table 3.28 Relationship between Cr(VI) concentration and integrated absorbance on the preconcentration system using KR

[Cr(VI)] (μg/l)	Integrated absorbance			Average	Average-blank	SD
Blank	0.001	0.001	0.001	0.001	0.000	0.000
0.005	0.004	0.002	0.003	0.003	0.002	0.001
0.010	0.018	0.015	0.017	0.017	0.016	0.002
0.050	0.032	0.030	0.035	0.032	0.031	0.003
0.100	0.043	0.042	0.057	0.047	0.046	0.008
0.250	0.093	0.095	0.094	0.094	0.093	0.001
0.500	0.190	0.183	0.185	0.186	0.185	0.004
0.750	0.287	0.285	0.287	0.286	0.285	0.001
1.000	0.392	0.374	0.377	0.381	0.380	0.010
1.250	0.463	0.472	0.468	0.468	0.467	0.005
1.500	0.646	0.647	0.645	0.646	0.645	0.001

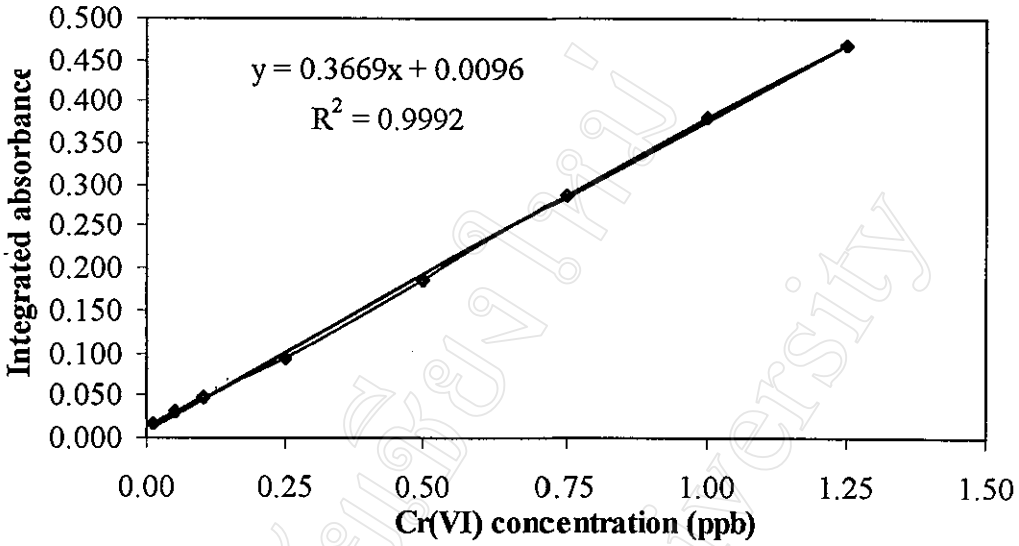

Figure 3.27 Calibration curve of Cr(VI) for the FI on-line preconcentration system using knotted reactor

Table 3.29 Relationship between Cr(VI) concentration and integrated absorbance on the preconcentration system using PTFE beads packed column

[Cr(VI)] (μg/l)	Integrated absorbance			Average	Average-blank	SD
Blank	0.065	0.067	0.066	0.066	0.000	0.001
0.005	0.065	0.067	0.072	0.068	0.002	0.004
0.010	0.081	0.083	0.087	0.084	0.018	0.003
0.050	0.106	0.108	0.107	0.107	0.041	0.001
0.100	0.140	0.138	0.136	0.138	0.072	0.002
0.250	0.228	0.220	0.234	0.227	0.161	0.007
0.500	0.378	0.379	0.373	0.377	0.311	0.003
0.750	0.558	0.553	0.556	0.556	0.490	0.003
1.000	0.771	0.752	0.788	0.770	0.704	0.018
1.250	0.803	0.815	0.820	0.813	0.747	0.009

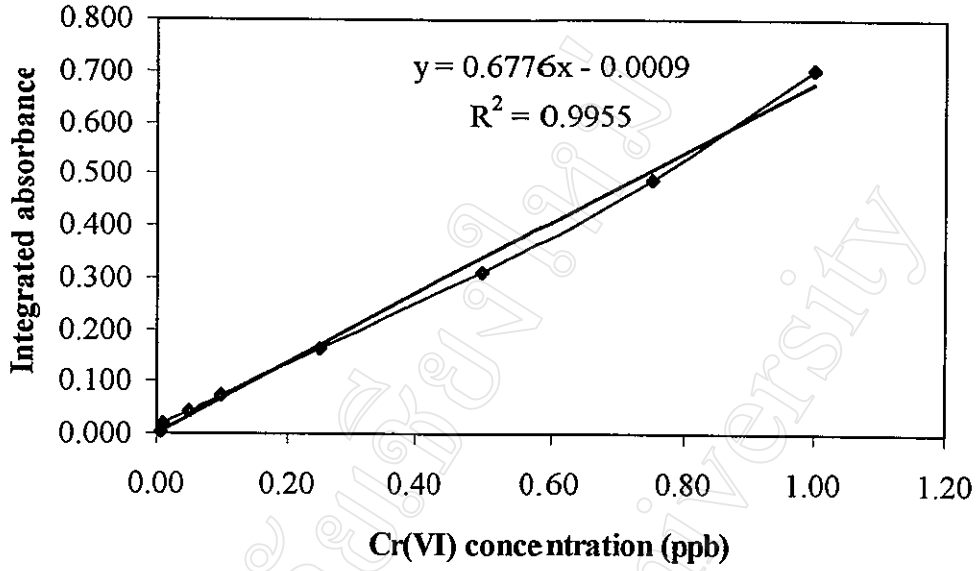

Figure 3.28 Calibration curve of Cr(VI) for the FI on-line preconcentration system using PTFE beads packed column

The limit of detection based on the analyte concentration which gives the response signal 3 times that of the standard deviation (3σ) of the blank plus response signal for the preconcentration system using the KR and the packed column was then calculated and illustrated in Table 3.30.

The repeatability of the system was investigated by making eleven consecutive runs with standard Cr(VI) of 0.50 μg/l for both the systems using the KR and the packed column. The results are shown in Table 3.31.

Table 3.30 Signal of reagent blank for detection limit calculation

Preconcentration unit	Blank signal	S.D.	3*SD	Regression equation	Detection limit (ng/l)
KR	0.002, -0.002, -0.002, -0.003, -0.001, 0.001, 0.001, -0.001, 0.002, -0.001, -0.004	0.005	0.015	Y=0.3669X+ 0.0096	**16.0**
Packed column	0.066, 0.063, 0.067, 0.062, 0.068, 0.064, 0.066, 0.067, 0.067, 0.065, 0.063	0.002	0.006	Y = 0.6776X- 0.0009	**9.0**

Table 3.31 Repeatability for Cr(VI) determination

Preconcentration unit	[Cr(VI)] (µg/l)	Integrated absorbance	Average	S.D.	%RSD
KR	0.50	0.190, 0.183, 0.185, 0.178, 0.190, 0.183, 0.185, 0.178, 0.177, 0.185, 0.183	0.183	0.004	**2.40**
PTFE beads packed column	0.50	0.378, 0.373, 0.379, 0.371, 0.369, 0.372, 0.378, 0.373, 0.379, 0.371, 0.369	0.374	0.004	**1.05**

The characteristic performance data obtained by using both the packed column and the KR were summarized and compared in Table 3.32.

Table 3.32 Performance of the FI-ETAAS on-line sorption preconcentration systems incorporating a PTFE KR or a column reactor packed with PTFE beads for the dertermination of Cr(VI)

Parameter	Preconcentration unit	
	Knotted reactor	**PTFE beads packed column**
Sample flow rate (ml/min)	5	5
Calibration range (μg/l)	0.01-1.25	0.005-1.00
Regression equation (eight standards, n=3)	0.3669[Cr(VI)]+0.0096 (corr. = 0.9992)	0.6775[Cr(VI)]-0.0008 (corr. = 0.9954)
Sampling frequency (*f*) (sample/h)	16.7	16.7
%RSD (n=11; 0.5 μg/l)	2.4	1.1
Limit of detection (3σ) (ng/l)	16	9
Enrichment factor (EF)	16.3	30.1
Concentration efficiency (CE=EF*x*/60)	4.5	8.4
Retention efficiency (%)	13.1	24.1

The advantages of the proposed packed column over the KR were notably in terms of limit of detection, enrichment factor and retention efficiency. The limit of detection (3σ) was enhanced by a factor of 2 when the column reactor was used, yielding a detection limit as low as 9.0 ng/l. The enrichment factor and the retention efficiency were calculated from the ratio of the slope of the calibration curves with and without a preconcentration step, respectively. Without preconcentration, 40 μl of a Cr(VI) solution was introduced directly into the graphite tube. The enrichment factor was increased nearly twice, from 16.3 to 30.1. In terms of retention efficiency, it was found that this parameter exhibited a rather low value for both the KR and the packed column reactor. Therefore, a recently proposed method based on so-called multiplexed sorption was tested for improving the efficiency of complex retention on the sorbent material [118]. Thus, Yan *et al.* found that FI on-

line multiplexed sorption preconcentration was beneficial for sorption of a Pb-PDC complex in a KR. In contrast to conventional FI preconcentration, the multiplexed preconcentration approach divides a single longer preconcentration step evenly into several shorter sub-steps while the total preconcentration time is kept constant. In their work, this proposed method was found to improve the preconcentration efficiency by a factor of 2. This was explained by a more efficient adsorption and better uniform distribution of the Pb-PDC complex onto the inner wall of the KR.

Although most intriguing, similar results were not obtained when using this approach for the present assay. Thus, when dividing the total preconcentration time of 60 s into four sub-preconcentration step, no significant improvement in preconcentration efficiency was observed as compared with the conventional single continuous sample loading. This might be due to a lower retention efficiency of the Cr (VI)-PDC complex on the PTFE material at the low concentration levels of Cr(VI) used in this investigation. Possibly, the proposed multiplexed sorption preconcentration procedure might merely be applicable for metal-PDC complexes at high concentration levels. In addition, further investigations are required to illuminate this point.

Although the retention efficiency of the Cr(VI)-PDC complex in this work was rather low for both the KR and PTFE beads packed column reactor, a two-fold enhancement in retention efficiency was, nevertheless, observed for the packed column.

The improved results in terms of limit of detection, enrichment factor and retention efficiency indicate that a higher preconcentration efficiency can be achieved with the proposed packed column as compared to the KR, comparing

preconcentration units of equal total surface area of adsorption. Notably, the detection limit exhibited of the present column is superior to those reported for the preconcentration of Cr(VI) on packed column using other sorbent materials which can be shown in Table 3.33.

Table 3.33 Characterisitc performance of the preconcentration system using a packed column for determination of Cr

Samples	Species	Sorbent	Technique	Detection limit (μg/l)	Ref.
Estuarine, coastal water	Cr(III), total Cr	Immobilizes quinoline-8-ol, Muromac A-1	FI-FAAS	6.0 (Cr(III)) 2.0 (Cr(VI))	24
Waste water	Cr(III), Cr(VI)	Amberlite IR-120, Amberlite IRA-400	FI-FAAS	14.3 (Cr(III)) 1.4 (Cr(VI))	25
Natural, tap, mineral, river water	Cr(III), total Cr	Chelating reisn (PAPhA)	FI-FAAS	0.2 (Cr(III))	26
Sea water	Cr(III), Cr(VI)	C_{18} bonded silica gel	FI-FAAS	0.02 (Cr(III)) 0.02 (Cr(VI))	27
Surface water	Cr(VI)	Solid DPC	FI-spectro.	5.0	29
Tap water	Cr(III), Cr(VI)	Chelex-100 resin	FI-FAAS	2.0 (Cr(III)) 2.0 (Cr(VI))	31
Surface water	Cr(III), Cr(VI)	RP-C_{18}	LC-FAAS	24.0 (Cr(III) 75.0 (Cr(VI))	36
Drinking water, urine	Cr(III), Cr(VI)	RP-C_{18}	FI-FAAS	0.92 (Cr(III)) 0.54(Cr(VI))	37
Drinking, river, lake water	Cr(III), Cr(VI)	Activated alumina	FI-FAAS	1.0 (Cr(III)) 0.8 (Cr(VI))	39
Sea, lake, drinking water	Cr(VI), total Cr	RP-C_{18}	FI-ETAAS	0.016 (Cr(VI)) 0.018 total Cr	77
Drinking, surface, ground water	Cr(VI)	RP-C_{18}	FI-spectro.	0.02	96

Table 3.33 (continue)

Samples	Species	Sorbent	Technique	Detection limit (μg/l)	Ref.
UHT milk	Cr(VI), total Cr	Chromabond NH_2	ETAAS	0.15 (Cr(VI)) 0.20 total Cr	97
Natural water	Cr(VI)	Activated alumina	FI-spectro.	0.20	98
Natural water, sediments	Cr(VI)	PTFE turnings	FI-FAAS	0.80	109
Certified waters	Cr(III), Cr(VI)	Activated alumina	FI-ICPAES	1.40 (Cr(III)) 0.20 (Cr(VI))	119
Pond waters	Cr(III), Cr(VI)	RP-C_{18}	HPLC-FAAS	0.04 (Cr(III)) 0.08 (Cr(VI))	120
Natural waters	Cr(III), Cr(VI)	Cellex-P, Cellex CM, Chelex-100	FI-FAAS	0.78 (Cr(III)) 1.40 (Cr(VI))	121
River waters	Cr(III), Cr(VI)	Polymeric Detata	ETAAS	0.03 (Cr(III)) 0.03 (Cr(VI))	122
Certified fresh water	Cr(III), Cr(VI)	Dionex AS4A	IC-chemilum.	0.05 (Cr(III)) 0.10 (Cr(VI))	123
Lake, waste, tap water	Cr(III), total Cr	Sodium dodecyl sulphate coated alumina	ETAAS	0.57 (Cr(III)) 0.35 total Cr	124
Waste waters	Cr(III), Cr(VI)	Waters IC-Pak A, waters Guard-Pak CM/D	IC-ICPMS	0.30 (Cr(III)) 0.50 (Cr(VI))	125
Certified natural water	Cr(III), Cr(VI)	Dionex CG 5, Dionex AG 7	IC-chemilum.	0.12 (Cr(III)) 0.09 (Cr(VI))	126
Certified natural water, Cr(VI) speciation solution, synthetic seawater	Cr(VI)	PTFE beads	FI-ETAAS	0.008	This work

3.3.9 Investigation of Interferences

Since APDC potentially is a complexing agent for a large number of metals, interferences from coexisting metal ions always have to be considered in order to achieve a desired degree of selectivity. Thus, the effects of a number of representative potential interfering species, namely Cu(II), Cd(II), Zn(II), Pb(II), Ni (II), Co(II) and Fe(III), were tested with the proposed packed PTFE column. The effect of these ionic constituents on the determination of Cr(VI) was summarized in Table 3.34.

At a concentration level of Cr(VI) of 0.5 μg/l only Co(II) was found to interfere significantly. The tolerance concentration was found at 0.01 mg/l, which, in fact, is a level that potentially might be encountered in natural waters. However, any interference effects could be minimized by using the standard addition procedure for quantification. Using this approach, very satisfactory results were obtained for the determination of Cr(VI) in natural water and synthetic seawater samples.

3.3.10 Evaluation of the PTFE Beads Packed Column Preconcentration Procedure

The developed method was applied to analysis of Cr(VI) in a SRM NIST-2109, Cr(VI) speciation solution, a SRM NIST-1640, trace element in natural water, and a synthetic seawater, respectively, to verify its accuracy. All the determinations were performed by using standard addition for calibration. The results are given in Table 3.35.

Table 3.34 Investigation of the tolerance of potentially interfering ions when using the FI system incorporating the column reactor packed with PTFE beads

Interfering ion	Concentration (mg/l)	Recovery (%)
Cu(II)	0.050	96.4
	0.100	117.2
	0.300	199.2
Cd(II)	0.010	98.9
	0.050	97.3
	0.100	101.1
	0.300	84.4
Zn(II)	0.050	98.9
	0.100	103.2
	0.300	97.3
	0.500	39.5
Pb(II)	0.050	102.1
	0.100	109.3
	0.300	102.3
	1.000	102.2
	1.500	95.9
	2.000	96.8
	5.000	63.6
Ni(II)	0.010	92.9
	0.050	115.2
	0.100	150.1
Co(II)	0.001	106.5
	0.005	104.4
	0.010	102.9
	0.050	76.9
Fe(III)	0.010	114.9
	0.050	102.7
	0.100	76.2

The concentration of Cr(VI) was in all cases 0.5 μg/l. The effect was expressed as recovery for the levels added.

Table 3.35 Determination of Cr(VI) in a SRM NIST-2109, SRM NIST-1640 and a synthetic seawater sample, respectively, using the PTFE beads packed column

Sample[a]	Certified concentration	Cr(VI) found concentration [b] (μg/l)
NIST-2109	1000 ± 4 mg/l Cr(VI) diluted to 0.20 μg/l Cr(VI)	**0.216 ± 0.018**
NIST-1640	38.6 ± 1.6 μg/l total Cr diluted to 0.20 μg/l total Cr	**0.006 ± 0.003**
NIST-1640	38.6 ± 1.6 μg/l total Cr diluted to 0.20 μg/l total Cr and spiked with 0.20 μg/l Cr(VI)	**0.214 ± 0.007**
Synthetic seawater	Spiked with 0.20 μg/l Cr(VI)	**0.208 ± 0.009**

[a] The pH of the sample was adjusted to a level of 0.015 M HCl

[b] The determination was done within 95% confidence intervals (n = 3).

In all assays, standard addition was determined by adding 0, 0.1, 0.2 and 0.3 μg/l Cr(VI) to the sample.

As shown in Table 3.35, the results achieved from the NIST Cr(VI)-reference material were in good agreement with the recommended value. When analyzing the NIST-1640, no Cr(VI) content was found (0.006±0.003). This is due to the fact that the Cr-content in this sample is almost Cr(III) (see Section 3.2.12). This state was proved by spiking the sample with 0.20 μg/l of Cr(VI). A reasonable recovery of 0.214 μg/l of Cr(VI) was then found. Finally, a synthetic seawater sample spiked with Cr(VI) at a concentration level of 0.20 μg/l was analyzed. Again, a very satisfactory recovery was found. The packed column has proven to be most reliable for determination of Cr(VI).